Multifractal Scaling characteristics of lineament networks of a fractured sandstone aquifer system

Safia Abdi (s.abdi@lagh-univ.dz)
Amar Telidji University
Mohamed Chettih
Amar Telidji University

Research Article

Keywords: Multifractal analysis, 2D-MAFN, Fractures Network, Lineament, Fractured Aquifers, Saharan Atlas

Posted Date: September 14th, 2023

DOI: https://doi.org/10.21203/rs.3.rs-3320257/v1

Additional Declarations: No competing interests reported.

Version of Record: A version of this preprint was published at Earth Science Informatics on January 15th, 2024. See the published version at https://doi.org/10.1007/s12145-024-01222-9.

Multifractal Scaling characteristics of lineament networks of a fractured sandstone aquifer system

Safia Abdi[1]; Mohamed Chettih[1]

s.abdi@lagh-univ.dzm.chettih@lagh-univ.dz

[1]Research Laboratory of Water Resources, Soil and Environment, Department of Civil Engineering, Faculty of Civil Engineering and Architecture, Amar Telidji University, P. O. Box 37.G, 03000 Laghouat, Algeria

0000-0001-5626-6228 (ORCID ABDI S)

0000-0001-6814-1828 (ORCID CHETTIH M)

Abstract

In this work, we have shown that we can carry out a multifractal characterization of fracturing from a network of lineaments, using a calculation code that we have developed ourselves and that we have named: 2D Calculation Code for Multifractal Analysis of Fracture Networks (2D-MAFN). Four lineament maps at different scales were analyzed, corresponding to the Upper Jurassic and Cretaceous geological formations of the El Gada region in the Central Algerian Saharan Atlas.The geometric analysis of the lineament networks showed good consistency between the lineament networks and the geological structure of the Atlas Range and its fault network. It also showed that the distribution of the lengths of the lineaments fits the power law. This analysis also revealed that, on a larger scale, diffuse fracturing appears to be more prevalent. In addition, the spectral analysis, through the decrease in spectral power according to a power law, characterizes a self-similar behavior and already seems to prove the scale invariance of the lineaments.The fractal dimension values obtained reflect the extent of fracturing and the degree of complexity of the network of lineaments. These values show that the lineaments are also well correlated with each other. The partition functions show that the points line up on the adjustment lines according to a law characteristic of multifractal behavior. In addition, the curves of generalized dimensions as a function of moments show a clear decrease, highlighting the multifractal nature of the fracturing process. In addition, the multifractal spectra in the form of bell curves also confirm the multifractal process for the four lineament networks analyzed.The results obtained are very encouraging and open up the prospects of modelling fracture networks for a variety of purposes, including assessing the connectivity of a fracture network.

Keyword: Multifractal analysis, 2D-MAFN, Fractures Network, Lineament, Fractured Aquifers, Saharan Atlas

Introduction

The geometrical structure of the aquifers fissured is most often identified with the favor of the fracturing, this is why, the analysis of the fracturing became a major element of the study of the fissured mediums. Several different approaches were developed to apprehend the fracturing (Razack 1984; Ghosh and Daemen 1993; Gilman 2003).The first models intended to represent the fractured mediums date from the Sixties (Barenblatt et al. 1960; Warren and Root 1963). Thereafter, more specific models have contributed to the recognition of the fractured mediums (Gringarten and Ramey 1974; Gringarten et al. 1974; Cinco et al. 1975; Jenkins and Prentice 1982; Thiéry et al. 1983; Thrailkill 1988) but, they remained limited to the estimation of the hydrodynamic characteristics at the local scale.

Since these first models, the study of the hydraulic properties of the fractured mediums has greatly increased, in direct relationship with different problems related to the questions of safety for the implementation of underground storage sites for radioactive waste, for the study of the recovery of the fluids, for the assisted injection, for the prediction of the migrations of pollutants, or even for the geothermal energy production(Cacas et al. 1990; Olsson 1992; Hsieh et al. 1993; Neretnieks 1993; Shapiro and Hsieh 1996; Tsang and Neretnieks 1998; Witherspoon 2000). For these networks of fractures, which have complex geometrical properties, the heterogeneity of the hydrodynamic characteristics is directly related to the heterogeneity of the network structure (Darcel et al. 2003).The fractures that practically allow an increase in the permeability of the reservoir can be of different natures. These different types of fractures are distributed in a very heterogeneous way (Cowie et al. 1995; Ouillon et al. 1995; Bour and Davy 1999). These have complex geometric properties requiring appropriate tools for analysis (Verscheure et al. 2010).For certain authors (Bour and Davy 1999; Bonnet et al. 2001). Fracture networks allow to justify the use of the power law to describe certain characteristics of the network such as the length. The lognormal law can be also used to describe other types of fracturing having a characteristic scale, related to the thickness of the lithological units (Odling et al. 1999). In addition, for Lasm and Razack (2001); Liu et al. (2002); Srivastava et al. (2004); Razack and Lasm (2006); Mariethoz et al. (2010) it would be more interesting to use the tools of geostatistic for a spatial analysis of the fracturing, justified by typical and regular variograms. However, these statistical approaches do not effectively describe the spatial distribution of fracture networks which may have scale invariance properties. Thus, fractal and multifractal methods are particularly adapted to the study of the networks of fractures. The networks of fractures usually present a self-similar character; they seem identical to various scales of observations (Darcel et al. 2003; Weiss 2003). The self-similar aspect also leads to think that networks have a fractal character, which can be determined on the spatial distribution of the fractures (Potirakis et al. 2012; Zazoun et al. 2015; Pavičić et al. 2017; Wang et al. 2017; Basirat et al. 2019).

The generalization to the notion of multifractal essentially amounts to considering the multifractal sets as a hierarchy of sets of which each one has its own dimension fractal. Thus the multifractal formalism provides a scaling relation that requires a family, possibly infinite, of dimensions, rather than a single dimension as in the case of fractal geometry (LévyVéhel2000; Abry et al. 2002; Grazzini et al. 2007). The multifractal theory then offers a more appropriate framework for the study of these phenomena. (Mandelbrot 1974, 1975, 1982, 1989; Parisi and Frisch 1985; De Bartolo et al. 2004).

Thus, the objective of this work is to analyse the lineament networks of a fissured aquifer geological formation located in the Algerian Saharan Atlas using the multifractal approach and some related techniques to characterise the fracturing. The multifractal analysis will be carried out using a Matlab code that we have established ourselves and that we have named: 2D Computational Code for Multifractal Analysis of Fracture Networks (2D-MAFN) and which will be described using its flowchart showing the main functions.

The Saharan Atlas range by its position, dimension, altitude, lithology and structure is of great hydrogeological interest for the country. It represents a gigantic water tower containing important water reserves in the powerful fissured aquifer formations which, in turn, feed the hydrographic networks of the large Chotts of the High Plateaux and the large Chotts of the Sahara platform via multiple water sources.The terrain of the Saharan Atlas is mostly bare and devoid of vegetation, allowing good visibility of the crack networks from satellite images. The study area is an ideal terrain to test the methodology.

In its general context, this work is part of a research project on the modelling of fractured aquifers. As such, for these aquifers, flows are dependent on the connectivity of fractures considered as conduits (Adler and Thovert 1999; Berkowitz 2002; Huang et al. 2020b). The assessment of fracture network connectivity is very important in the design, evaluation and development of fractured reservoirs (Huang et al. 2020b). Connectivity can also be used as a very effective and efficient tool to predict potential flow paths and main drainage axes (Berkowitz 2002; Huang et al. 2020a).

Several methods have been suggested by different authors to assess the connectivity of a fracture network (Huang et al. 2020b). The analytical approach, based on percolation theory, is one of these methods, it focuses on the characteristics of random media and is applied in particular to formalise flow properties in complex media and for the modelling of certain natural phenomena. However, the evolution of fracture density across scales is most often fractal and the length distribution is power law (Davy et al. 1990; Bour and Davy 1999; Bonnet et al. 2001). This is likely to require a detailed analysis of the fracturing process and is the first step of the project and the objective of this paper.

Thus, the approach adopted in this work starts with a detailed description of the theoretical aspect of the fractal and multifractal analysis, and a description of the flowchart of the calculation code. Subsequently, the geological and structural context of the study area is briefly presented by describing the lithostratigraphic units of the study area and the major structural elements that characterise the geological formations. After a presentation of the data used in this study and the processing techniques, we will present the results obtained using spectral analysis, fractal analysis, as well as the geometric properties of the lineament networks. Finally, the results of the multifractal analysis will be presented and discussed by illustrating partition functions, mass exponents, generalized fractal dimensions and multifractal spectra of singularities.

Methodology

Theoretical aspect of fractal and multifractal analysis

The concept of fractal was introduced by Benoît Mandelbrot in 1975 with the aim to study objects that have a very irregular, fragmented or geometrically complicated shape (Mandelbrot 1975), although the first fractal example was introduced a century before by the mathematician Cantor (Cantor 1884). In addition, the multifractal geometry was introduced to describe the relations of scale between geometrical structures and the scale of analysis of these structures and to characterize these objects with the unusual properties in traditional geometry. It is thus a useful language to describe the complexe forms, and allows the description of nonlinear processes. The complexity of the shapes of the natural objects generally results from simple processes, often recursive. Thus it is thanks to computer science that the study of fractals has developed.

A fractal object is a mathematical object resulting from an iterative process and which presents a character of invariance of scale. The size of a fractal set varies as the scale to which it is examined, given by dimension fractal (Mandelbrot 1982;Wornell 1996). In reality, there does not exist any definition of the concept of fractal which is unanimously accepted. The definitions of dimension fractal, the self-similarity properties and auto affinity, help with the comprehension of this concept.

Fractal Dimension

The fractal dimension is above all a parameter allowing to quantify the complexity of a signal or an image. The fractal dimension is a generalization of the notion of whole dimension, specific to Euclidean geometry. There are various types: the dimension of auto similarity, the dimension of the Box Counting, the dimension of the compass, the dimension of Hausdorff, and the dimension of Minkowski-Bouligand.(Secrieru2009; Lausberg 1987).

For a structure fractal given, these dimensions in general provide values close to the theoretical value of dimension fractal. The algorithms most often used for the calculation of fractal dimension can be grouped in two principal classes (Lopes and Betrouni 2009): those known as of boxes counting (Russell et al. 1980), and those based on the fractional Brownian movement (Lausberg 1987).

The box-counting method is the first method developed to estimate the fractal dimension of an object (Russell et al. 1980). This method is the most frequently used and most popular. Note that this method is only valid for black and white images. The advantages of the technique of the boxes counting are the simplicity of its application and the direct estimation of the fractal dimension. Its general principle is to cover a signal with boxes of sizeε, if $N(\varepsilon)$is the number of boxes of size ε necessary to cover the object completely, the fractal dimension $D_f$is thus given by (De Souza and Rostirolla 2011):

$$D_f = \lim_{\varepsilon \to 0} \frac{\ln N(\varepsilon)}{\ln(1/\varepsilon)} \tag{1}$$

Multifractal Analysis

The description of the non-homogeneous geometrical structure of an object may require several fractal dimensions; this is called multifractality. The multifractal approach can be considered as an extension of the fractal theory (Evertsz and Mandelbrot 1992; Peitgen et al.2004). For some authors (Agterberg et al. 1996), the multifractals are fractals interlaced spatially with a continuous spectrum of fractal dimensions. The purpose of multifractal analysis aims is to study functions whose the regularity punctual may vary from one point to another (Arneodo and Jaffard 2004).The generalization of the notion multifractal essentially amounts to considering multifractal sets as a hierarchy of sets, each of which has its own fractal dimension (LévyVéhel 2000). A multifractal measure is related to the characterization of the spatial distribution of a quantity associated with a support (Feder 1988).Thus multifractal analysis provides a scale relationship that requires a family of dimensions (Abry et al. 2002). There are several ways to measure the local regularity of a signal (LévyVéheland Barrière2008). The first tools to measure regularity are: continuity, and derivability at a point (Arneodo and Jaffard 2004). Another tool, which has both solid theoretical foundations and intuitive content, is the use of Hölder exponents (LévyVéhel and Barrière 2008).

The numerical calculation of the spectrum of singularities of a signal is clearly impossible to perform directly from the theoretical definition (LévyVéhel2003;Arneodo and Jaffard 2004;Wendt et al. 2007). Thus, a technique known as multifractal formalism was established by Parisi and Frisch (Parisi and Frisch 1985) to calculate the spectrum of singularity. This formalism allows to establish a relationship between global and local behavior in the form of a transform of Legendre (Harte 2001).

Multifractal Formalism

The aim of multifractal formalism is to compute the spectrum of singularities not directly from Hölder's exponent definition, but rather from auxiliary quantities that can be easily estimated numerically (Arneodo and Jaffard 2004).

As in the case of estimation the fractal dimension, there are many methods to approximate the multifractal spectrum. The two principal methods are: the box counting method and the wavelet transform method (Arneodoet al. 1988; Mallat and Zhong 1991; Muzy et al. 1991; Bacry et al. 1993; Grassberger 1993; Arneodo et al. 1995; Gonzato 1998; Mallat1998; Turiel et al. 2006; Arneodo et al. 2008; Lopes and Betrouni 2009).

We define a measure μ on its supportS_{μ}. We then call the exponent of singularity at the point$x_0 \in S_{\mu}$, the limit:

$$\alpha(x_0) = \lim_{\varepsilon \to 0^+} \frac{\ln \mu(B_{x_0}(\varepsilon))}{\ln(\varepsilon)} \tag{2}$$

Where $B_{x_0}(\varepsilon)$designates a ball centered in $x_0$and of sizeε. The spectrum $f(\alpha)$of the singularities associated with the measure$\mu$is the function which, at allα, associates the fractal dimension of the set of points x_0 such as $\alpha(x_0) = \alpha$:

$$f(\alpha) = D_f\left(\{x_0 \in S_{\mu} / \alpha(x_0) = \alpha\}\right) \tag{3}$$

Where α is the Hölder exponent or Lipschitz-Hölder.

The $f(\alpha)$spectrum of singularities describes the statistical distribution of the exponents α on the support of the measurement. $f(\alpha)$ is a quantity which translates the degree of regularity or homogeneity of a fractal measurement. Thus, if one paves the support of the measurement of boxes of sizeε, Then the number of boxes whose measurement varies likeε^{α}, for a givenα, behaves as follows:

$$N(\varepsilon) \approx \varepsilon^{-f(\alpha)} \tag{4}$$

The multifractal formalism can also be related to a thermodynamic description of multifractal measurements. Consider the partition function, which for any$q \in \Re$,is written as:

$$Z(q,\varepsilon) = \sum_{i=1}^{N(\varepsilon)} \mu_i^q(\varepsilon) \tag{5}$$

Where the exponent q is a continuous real parameter $(-\infty < q < +\infty)$, which plays the role of order of the moment of measurement$\mu_i(\varepsilon)$. The partition function $Z(q,\varepsilon)$represents the sum of the moments of order q of the distribution of the measurement $\mu_i$on its support. The spectrum $\tau(q)$can then be defined from the power law behavior of $Z(q,\varepsilon)$when$\varepsilon \to 0^+$:

$$Z(q,\varepsilon) \sim \varepsilon^{\tau(q)} \tag{6}$$

Where the curve can be approximated by a straight line of slopeτ called the mass exponent$\tau(q)$:

$$\tau(q) = \lim_{\varepsilon \to 0^+} \frac{ln(Z(q,\varepsilon))}{In(\varepsilon)} \tag{7}$$

And we can also define the spectrum of generalized dimensions $D(q)$as the report:

$$D(q) = \frac{\tau(q)}{(q-1)} \tag{8}$$

The generalized fractal dimensions $D(q)$ are defined as the asymptotic behavior of the relationship between$ln(Z(q,\varepsilon))$ and $In(\varepsilon)$(Grassberger 1983; Halsey et al. 1986; Feder 1988;Olsen 1995;DeBartolo et al. 2004):

$$D(q) = \frac{1}{q-1} \lim_{\varepsilon \to 0} \frac{\ln(Z(q,\varepsilon))}{\ln(\varepsilon)} \qquad q \neq 1 \tag{9}$$

$$D(1) = \lim_{\varepsilon \to 0} \frac{\sum \mu_i(\varepsilon) \ln(\mu_i(\varepsilon))}{\ln(\varepsilon)} q = 1 \tag{10}$$

Where$D_0$is the fractal dimension, $D_1$is the information dimension and $D_2$is the correlation dimension and which correspond respectively to $q = 0, 1, 2$ (Grassberger 1983; Roux and Hansen 1990;Hirata and Imoto 1991; Cowie et al. 1995; De Bartolo et al. 2004).

The spectrum of singularities $f(\alpha)$, and the spectrum of generalized dimensions$D(q)$, are connected by a Legendre transformation (Feder1988). The multifractal spectrum characterizes the degree of regularity and homogeneity. It also describes the behavior of global quantities, i.e. statistical mean values of the$\mu_i$measure on the support (Feder 1988).

The Multifractal formalism using the box method enables to determine the Lipschitz-Hölder exponent and the multifractal spectrum from the Legendre transform. (De Bartolo et al. 2004):

$$\alpha(q) = \frac{d}{dq}[(q-1)D(q)] \tag{11}$$

$$f(\alpha(q)) = q\alpha(q) - (q-1)D(q) \tag{12}$$

The dimension D_0(for$q = 0$) of the spectrum of generalized dimensions is equal to the dimension of the physical support, which may itself be fractal, but not necessarily. In addition, if $D(q) = D_0$ for any value of$q$, it means that the measurement is uniform on the support, which corresponds to the definition of a classical fractal, or monofractal.

The curve$f(\alpha)$is a bell-shaped function for a multifractal signal, while it will be reduced to a point for a monofractal signal. The maximum value, located at the top of the bell, gives the fractal dimension of the support. Several parameters can be deduced from the multifractal spectrum such as curvature and width $\Delta\alpha$ that corresponds to the difference between the two ends of the spectrum.

Flowchart and Calculation Code

The simplified flowchart shown in Fig.1 presents the main steps of the 2D-MAFN calculation code. The first step is to read the image, read the moment order (q) and choose the scales corresponding to the sizes of the boxes (ε). The image transformed into binary code reveals its dimensions. The order of moment (q) corresponds to a continuous real parameter; it was taken in our calculations varying from -20 to 20 to have a broad vision on the variability of the process. We have taken the size of the boxes as successive powers of two.

The next step is to partition the image, dividing it into square boxes of different sizes (16, 32, 64, 128, 256, and 512). After calculating the total number of pixels, for each box size, the number of boxes needed to cover the image will be counted. This process generates a set of scaling exponents that will describe the relationship between the size of the boxes and their number. We then proceed to the determination of the measure $\mu_i(\varepsilon)$ and the calculation of its probability $P(i)$to finally arrive at the calculation of the partition function$Z(iq, i\varepsilon)$.

The following step allows the calculation of the mass exponent $\tau(i)$ which is simply the slope of $\log\big(Z(i,:)\big)$with respect to$\log(\varepsilon)$.

The generalized fractal dimensions $D(q)$ are calculated as a function of $\tau(q)$ and q using the expressions given by $\alpha$and$f$.

The last step calculates the multifractal spectrum by the Legendre transform where $\alpha$and f have already been calculated in the previous step.

Geological and structural context of the study area

General geological framework

The geological history of the Maghreb sedimentary basins is part of a process of global geodynamics of plate tectonics in North Africa (Fig.2). This process has structured Algeria into three distinct geological domains:

- An allochthonous domain called the Tellian domain corresponds to alpine nappes ;
- A strongly pleated domain corresponding to the Atlas domain and to a tabular sector attributed to the high plateaux ;
- A slightly deformed area of the foreland of the Alpine range representing the Sahara platform.

Tellian Domain

The Tellian domain consists of the most northern allochthonous sets of West North Africa. This area corresponds to the thrust slicks sets relayed towards the North-East by the European Calabro-Sicilian Arc. The Algerian Tellian domain is subdivided into two: the northern Tellian Atlas and the southern Tellian Atlas.

- The northern Tellian Atlas corresponds to the internal zones of the Alpine range, it is formed by the massifs of Kabylia which corresponds to a carted basement, formed of Precambrian, metamorphosed and granitized Paleozoic terrains, often of complex structure. On this basement, the Mesozoic to Eocene sedimentary cover, itself nested in small layers, forms the limestone chain. The latter is surmounted by thick series of flyschs in an allochthonous position as well. The northern Tellian domain largely overlaps towards the South the following domain;
- The southern Tellian Atlas corresponds to the area of the Tellian nappes which are rooted to the south of the Kabyle massifs. These layers are often dandruff and their establishment from the North to the South in the Miocene was favored by the presence of an argilo-evaporite formation of the Upper Triassic (Vila 1980). They originate from the interweaving of thick Mesozoic to Cenozoic series deposited in the tellian furrow that corresponded to a subsidence zone.

Atlas domain and high plateaux :

The Atlas domain is an intra-continental mountain range, commonly called the Saharan Atlas. It corresponds to a succession of highly fissured clay-sandstone and carbonate formations, structured essentially during the Alpine cycle. In the Saharan Atlas, the geological framework comes mainly from tertiary folds. The Jurassic and Cretaceous series, which constitute the basic structure of the Mounts of Ksour, Jebel Amour and the Mounts of Ouled Nails have been quite energetically folded, in a general direction South-West North-East. The folding of the Saharan Atlas occurs at the Cenozoic, mainly during the Atlas compressive phase dated to the Eocene (Laffitte 1939).This tectonic phase was followed by post-Pliocene movements, also compressive (Laffitte 1939; Vila 1980; Ghandriche 1991). As for the ante-eocene structural inheritance, it is represented by distensive tectonic phases essentially at Lias and Cretaceous (Guiraud 1975; Vila 1980; Aissaoui 1984; Bureau 1986).

The sediments that were deposited in the Atlas furrow during the Secondary are characteristic either of neritic and shallow marine environments, or of continental or lagoon environments. The large masses of Mesozoic sediments in such sedimentary environments cannot be explained without involving the play of subsidence. The folds continued with the sinking of the folded structures. Thick reddish detrital series filled all the tertiary depressions. The first sedimentary deposits and the first generation of quaternary forms interlocked, before the tectonic movements were completely finished.

The high-plateaux domain is interposed between the Atlas and Tellian domains, and constitutes the Alpine foreland, with reduced sedimentary cover, where local distension processes have allowed the formation of certain intramontane basins. However, in the East, you can see the absence of high plateaux, located at the front of the Tellian nappes, the Eastern Saharan Atlas is classically considered as a foreland of the alpine chain of North Africa.

Sahara platform

It is located in the south of alpine Algeria and belongs to the North African Craton. It includes a Precambrian base on which rests in discordance a powerful sedimentary cover, structured at the Paleozoic in several basins separated by high zones. The north-eastern part of the Sahara platform behaves in a high zone during the Mesozoic (Boudjema 1987), then sinks into the Neogene (Kazi-Tani 1986). This depression corresponds to the Melrhir Chott area. In this region, located at the edge of the Saharan Atlas, the effects of the Austrian phase (ante-Aptian) which are clearly marked on the Sahara platform, diminish considerably. On the other hand, the effects of the alpine phases, which are hardly noticeable towards the South, are widely manifested there. This results in the reorientation of faults and previous structures (Boudjema 1987). The transition from the Atlas domain to the Sahara platform is highlighted by the South-Atlasic accident that extends from Agadir to the Gulf of Gabès. It is in fact a band formed by a series of faults and flexures, relaying from West to East. It constitutes a sedimentary limit with significant change in facies and a tectonic boundary, between an Atlas domain that rises since the Neogene and a South-Atlasic pit that widens since the Miocene (Laffitte1939; Cornet 1959; Caire 1975; Busson 1970; Guiraud1973; Aissaoui 1984;Kazi-Tani 1986; Frizon de Lamotte et al. 1990).

Geological aspect of the study site

The study area is the El Gada region of Jebel Amour located 100 km northwest of the city of Laghouat. The geological map of the study site (Fig.3) shows a succession of anticlinal and synclinal folds in relays roughly oriented North-East South-West.

Lithostratigraphy

In this part of the Saharan Atlas, the geological formations of the Middle and Upper Jurassic constitute a thick series of more than 2000 m of varied lithology representing several mega-sequences mainly linked to the reactivations of the tectonic subsidence. The basal sandstone formations of the region have been attributed to the Dogger, while higher in the series, appears a carbonate set attributed to the basal Kimmeridgian.

The roof of the series has been dated Portlandian-Berriasian, while for the rest of the series some facies fossils allow a more or less questionable attribution to the lower or upper Kimmeridgian in the limestone layers. The Cretaceous stratigraphic unit consists of a first set of dolomitic and evaporitic limestone from the Upper Albian to the Senonian, and a second set of sandstone with quartz dragees attributed to the Upper Berriasian to the Lower Albian.

The Continental Tertiary marks a return to continental sedimentation, and it thus designates very diverse formations in facies and thickness, the most common facies of which is that of a red sandy clay sediment.

The Quaternary morphological evolution consisted mainly in the progressive clearing of the atlasic structures. This stage began with the shaping of a system of glacis. It ended with the formation of low terraces along the main wadis.

Structural elements

The central part of the study area is mainly characterised by a vast syncline drawn in the Lower Cretaceous quartz-dredged continental formations. It corresponds to the El Gada syncline, narrow to the North-East at the level of Djebel Zeïreg, where it is affected by a network of conjugated faults. It spreads out towards the south-west in a vast plateau formed by sub-horizontal dipping sandstones deeply dissected by erosion.

Further north of the syncline, the relief of Jebel Zlarhis made up of the structurally highest part of the anticline, where the Kimmeridgian sandstones form an anticlinal vault affected by transverse faults marked out by Triassic injections. On the south-western periclinal of Jebel Zlarh, the depression of Aîn El Harfi draws a circular shape with straightened sides interpreted as a diapiric rise of the Triassic represented by red and purple clays and silts, by dolomites and green rocks of volcanic origin.

Further south, the Kef Mimouna anticlinal zone corresponds to the termination of the anticlinal area where the Dogger outcrops. The Oxfordian sandstone series show themselves to be affected by multiple breaks and folds. It appears that a late phase of distension had caused a collapse of the axis of the anticline fold resulting in these structures. In the South-East of the map, appears the syncline of El Hadjeb, characterized by a very flat and little marked topography where the dips are weak and where the limestones of the Portlandian undoubtedly not very deep. It corresponds to the extension of the perched syncline of Djelfa with a upper Cretaceous core in the North-East. Quite to the South-East of the map appears an anticlinal structure corresponding to the Dome of Tadjmout in the Portlandian clay-gypsum crossed in the center by a set of shearing faults.

In the North-West, bordering the anticline axis of Jebel Zlarh is the synclinal area of Aflou-Jebel Gourou. In the southwestern part, the syncline is formed by sandstone with quartz dragees from the Lower Cretaceous, further North-East, the syncline is made up of a formation of dolomitic limestones to the Djebel Gourou attributed to the Upper Cretaceous. The syncline is limited to the North-West by an important singular accident, which presents itself as an undulating anticlinal axis in plan, very acute in cross section with flanks formed by terrains often of different ages following the same transverse. Triassic points related to the diaper mark the accident in the North of Djebel Gourou and in the South of Djebel SidiOkba.

The geological map highlights three major fault directions:

- The direction North 50 to North 60, it most often corresponds to sinistral strike-slip faults ;
- The direction North 150 to North 160, oblique to the axes of the folds, corresponds to the faults which appear in dextral strike-slip faults ;
- For the North 110 to North 120 direction, these are normal and reverse faults and dextral strike-slip faults.

We can also note a fourth orientation family of submeridian secondary importance.

Data

The database used in this study includes Landsat-TM satellite images, the 1/200 000 geological map of Laghouat and the results of structural measurements obtained during our field investigation campaigns. Thus, the analysis is based on the processing and interpretation of a Landsat 7 ETM+ Path 196 and Row 36, multispectral and panchromatic scene covering the study area (Fig.4).

However, given the scale invariance properties that could characterise lineament networks, we opted for four satellite images covering the El Gada region at different scales (Fig.5).As such, we have chosen the following scales: 1/200 000; 1/100 000; 1/50 000 and 1/25 000.

The image processing consists of lineament identification and extraction. The processing was carried out using ENVI software for color compositions, principal component analysis and directional filters. Directional filters of the 7 X 7 Sobel matrix type were applied in the N 0°, N 45°, N 90° and N 135° directions.

The structural nature of the lineament network was subsequently validated by eliminating all straight lines related to anthropogenic activities and those of the hydrographic network. In addition, the geological investigations carried out during our various field campaigns were also used to compare the results obtained. Finally, the resulting synthetic lineament maps are presented in Fig.6.

Results and discussion

Preliminary analyses

On the one hand, preliminary analyses are necessary in order to show that the characteristics of the lineament networks are entirely consistent with our field observations. Secondly, these analyses will gradually enable us to justify the adoption of fractal and multifractal analyses to characterise the lineament networks. To this end, a quantitative analysis of the geometry of the network of lineaments was briefly carried out in this study to determine the rose diagrams of the lineaments and their histograms of the orientation angles, as well as the histograms of the length frequencies and their fit to a power law. A spectral analysis has also been included in this section because scale invariance is often reflected in the spatial form of the calculated statistics as spectral power, at least for moments of order 2.

Geometric analysis of lineament networks.

Quantitative analysis of the lineament networks enabled us to draw up rose diagrams for the four lineament maps (Fig.7) For scales of 1/200 000, 1/100 000 and 1/50 000, the rose diagrams clearly show the main North 50 - North 80 direction, corresponding to the North-East South-West direction of the Atlas range linked to the major Pyrenean tectonic phase, the main faults of which acted as senestial strike-slip faults. A second direction of lineaments of lesser importance, North 100 - North 130, corresponds to the class of North-West South-East faults and the major dextral strike-slip faults visible on the geological map.There is also a third, narrower, submeridian class, which appears to be emerging but remains below 5%, corresponding to the north-south faults on the geological map. These fractures are linked to the late Plio-Quaternary tectonic phase of submeridian shortening.

However, for the 1/25 000 scale lineament map, the rose diagram shows a fairly homogenous directional distribution with a very slight dominance in the two perpendicular directions North-East South-West and North-West South-East.The first corresponds to the direction of the Atlas range and the second corresponds to the normal and reverse faults and dextral strike-slip faults visible on the geological map.At this scale, the network of lineaments essentially corresponds to the small diffuse fractures which seem to predominate and which play an important hydrogeological role.

Histograms of orientation angles (Fig.7) clearly show a large majority of lineament classes oriented North-East-South-West at scales of 1/200 000, 1/100 000 and 1/50 000.However, for the 1/25 000 scale lineament map, there are two main classes of roughly perpendicular lineament running North-East South-West and North-West South-East.

The histograms of length frequency show an asymmetric distribution (Fig. 7).For many authors, including Long and Billaux (1987); Dverstop and Andersson (1989) and Cacas et al. (1990), the lognormal distribution is the most commonly used. However, studies carried out by Bonnet et al. (2001); Bour and Davy (1999) and others have shown that a power law distribution is better suited to representing the distribution of fracture network lengths. The value of the exponent$a$ of the power law ($n(l) \propto l^{-a}$) indicates the proportion of small fractures to large ones.The power law was tested to adjust the fracture length distribution (Fig.7).We used maximum likelihood estimators to fit the distribution.The slope values a obtained for the four lineament maps 1/200 000, 1:/100 000, 1/50 000 and 1/25 000 are 2.8914, 3.0199, 3.3475 and 5.8593 respectively, showing a predominance of short lengths and diffuse majority fracturing.

Spectral analysis

Scale invariance is translated on the spatial form of the statistics calculated on the signal. such as spectral power and autocorrelation function. It then appears that the notion of scale invariance is intimately linked to the spectra known as in $1/f$ and can be associated with the concept of fractal (Mandelbrot 1982). This simple analysis justifies in particular the emergence of the laws of power in the problems with invariance of scale. It thus emerges that spectral power follows a power law where we speak of self-similar behavior. Often, we are satisfied to consider the existence of behaviors in laws of scale in the statistics of order 2 only and one checks the adequacy with a spectrum in $1/f$. This property is mainly highlighted and is verified on the power spectrum alone; experimentally it is statistically observed that the spectral power presents a decrease in law of power (Field 1987 ; Turiel et al. 2005 ; Grazzini et al. 2007 ; Grazzini and Soille 2009) :

$$\Gamma_I(\vec{v}) \propto |\vec{v}|^{-\beta} \tag{13}$$

Where Γ_I is the spectral power, $\beta$the spectrum exponent and where $|\vec{v}|$ is the radial frequency. This translates into by a linear relationship between $Log\left(\Gamma_I(\vec{v})\right)$ and$Log|\vec{v}|$. The slope of the straight line obtained is *-β.* The goal of spectral analysis is practically to verify if the property of scale invariance exists, at least with regard to the order two.

Fig.8 illustrates the scale invariance on the power spectrum using the power spectral density in log representation and log-log diagram.

The results obtained from the power spectral density in log-representation clearly highlight the frequencial and angular characteristics of lineaments for maps at different scales. The presentations of the spectra of power in 2D also make it possible to determine the energy distribution of the image, to bring information on the periodicity and the orientation of the reasons for the texture of the lineaments. For the maps on the scale 1/200 000 and 1/100 000, we note rather periodic textures in the direction of the principal directions of the lineaments described previously and the concentrations of energy around the main axes. On the other hand, for linear maps at scales 1/50 000 and 1/25 000, the textures are globally rather homogeneous without privileged directions. The log-log diagrams of the spectral power present a clear decrease in power law characteristic of a self-similar behavior. The exponents of the β spectra obtained for the linear maps at scales 1/200 000, 1/100 000, 1/50 000 and 1/25 000 are respectively: -1.0865, -0.9653, -0.9343 and -0.8224. These values already seem to prove the scale invariance of the lineaments for the studied lineament maps.

Fractal Analysis

In reality, the determination of the fractal dimension using the box-counting method is abundantly documented in the literature (Allegre et al. 1982 ; Chilès 1988 ; Davy et al. 1990 ; Marrett and Allmendinger 1991 ; Gauthier et Lake 1993 ; Odling 1992 ; Walsh and Watterson 1993 ; Barton 1995 ; Castaing et al. 1996 ; Berkowitz and Hadad 1997 ; Bour and Davy 1999 ; Bonnet et al. 2001 and Darcel et al. 2003). Among the main advantages of the method it is that it can be applied for structures missing the property of strict autosimilarity, and that it can also be used for multifractal analysis, thus, for the facility of its programming.

The application of the box-counting method to the four lineament maps it allowed to have the results presented below. We have taken the box sizes as successive powers of two. Table 1 summarizes the results of counting and Fig. 9 illustrates the number of non-empty boxes as a function of box size, and one thus determines the slope of the graph by adjustment which is not other than Fractal Dimension D_f of the relation (1). The values obtained for the fractal dimension range from 1.86 to 1.88, they reflect the importance of fracturing and the degree of complexity of the fracture network. The Fig. 10, show the dimensions fractals calculated for each of the four linear maps, they are stable and significant values and that the fractures beautiful and are well correlated between them.

Multifractal Analysis

The box counting algorithm was applied for the four lineament maps to describe each iso-fractal subset by the generalized dimensions $D(q)$ and by the multifractal spectrum $f(\alpha)$. Thus, the partition functions $Z(q,\varepsilon)$ of equation (5) for the four lineament maps were constructed for values of q ranging from -20 to 20. The partition functions of the four lineament maps are presented in Fig. 11. It is practically noticed that all the points are aligned perfectly on the adjustment lines. Thus, the data follow a power law characteristic of multifractal behavior and this for all the range of scale. The scale invariance property already detected on the Fourier power spectra is confirmed by the behavior of the moments.

From the partition function and for each q, the mass exponent $\tau(q)$ can thus be considered as the slope obtained on the logarithmic representation of $Z(q)$ compared to the representation logarithmic of ε. On scales where Z presents a power law behavior, $\tau(q)$ in general presents curves with very low convexity characterizing the scale invariance indicating the asymptotic behavior of the moments of order q.

Thus, for different values of q, ranging from -20 to 20, and by calculating the function $\tau(q)$ according to the equation (7), we obtained the curves presented in fig.12. We note that the curves obtained for the four lineament maps are practically superimposed, and that the weak convexity characterizing the scale invariance is not clearly highlighted to decide.

As such, it is more interesting to see the variations of the generalized dimensions $D(q)$ as a function of q as it was presented in paragraph 3. Fig. 13 shows the variations of the generalized fractal dimensions $D(q)$ as a function of q for values of q ranging from -20 to 20. The curves obtained show clearly the decrease of $D(q)$ when q increases and put this ahead and clearly the multifractality of the process for the four linear maps. Indeed, a monofractal process would have only one fractal dimension and would have only one constant value of $D(q)$, whatever of q.

The multifractal spectrum of the singularities $f(\alpha)$characterizes the degree of regularity and homogeneity of the process.Thus,the multifractal spectra are estimated from the Legendre transform for the four lineament maps (Fig. 14).The results obtained show multifractal spectra in the form of bell-shaped curves confirming the multifractal process of the lineament distribution.The maximum of the curves being equal to 2 thus giving the fractal dimension of the support.

This analysis allowed showing that the process of the distribution of the lineaments at least for the four scales chosen is a multifractal process, this can be extrapolated on larger scales in order to characterize the geometry of the fracture networks and to guide future development work.

Conclusion

This study has allowed to show that from simple satellite images, it is possible to carry out thorough analysis of the fractures networks. In this respect, the geometric analysis of the lineament networks showed the analogy and strong similarity between the lineament network and the fractures mapped on the geological maps. It has also shown that the distribution of lineament lengths can be easily fitted to a power law. In addition, spectral analysis of the lineament networks revealed fairly periodic textures along the main directions of the lineaments and energy concentrations around the main axes, but on a larger scale, the textures are fairly homogeneous overall, with no preferred directions, where diffuse fracturing seems to be in the majority.

However, in general, the spectral power shows a clear power-law decay characteristic of self-similar behavior, which seems to prove the scale invariance of the lineaments for the lineament networks analyzed. The fairly high fractal dimension values obtained reflect the extent of fracturing and the degree of complexity of the lineament network, and a priori indicate the existence of many degrees of freedom.

For multifractal analysis, the partition functions show that the points are aligned on the fitting lines following a power law characteristic of a multifractal behavior. In addition, the low convexity of the curves of the mass exponents did not allow to clearly highlighting the scale invariance. However, the curves of the generalized dimensions as a function of the moments show clearly a decrease highlighting the mulifractality of the process. In addition, the multifractal spectra in the form of bell curves confirm the multifractal process of the lineament distribution for the four networks analyzed.

Ultimately, the methodology adopted represents a very powerful, flexible and reliable tool for the multifractal characterization of fracture networks and opens up the prospect of modelling attempts to assess the connectivity of fracture networks.

Declaration

Safia Abdi, Ph.D candidate
E.mail: s.abdi@lagh-univ.dz

Research Laboratory of Water Resources, Soil and Environment, Department of Civil Engineering, Faculty of Civil Engineering and Architecture, Amar Telidji University, P. O. Box 37.G, 03000 Laghouat, Algeria.

September 2023.

I, the undersigned Ms. Safia Abdi, declare on my honor that the work presented in the submission for publication in the journal Earth Science Informatics is a personal work carried out as part of my doctoral thesis under the supervision of Professor Mohamed Chettih and that we contributed together to the conception of the article and that we take full responsibility together for everything presented in the article.

Furthermore, I also declare that the work presented in the submission for publication in the journal Earth Science Informatics is not affected by any conflict of interest.

However, I would like to clarify that our work is part of a doctoral training project in which there is no where there is no funding to declare.

I would also like to state that the data used in the treatment of this work are those of the authors (Abdi S. & Chettih M.) and that there is no specific material to report.

Finally, I also declare that I Safia Abdi is the only correspondent with the editor of Earth Science Informatics as far as our article is concerned.

Please accept my most distinguished greetings.

S. Abdi

Ph.D candidate

References

Abry P, Gonçalves P, Lévy Véhel J (2002) Lois d'échelle, fractales et ondelettes. Hermès Sciences Publications. https://hal.inria.fr/inria-00570634

Adler PM, Thovert JF (1999) Fractures and fracture networks .Springer Science & Business Media.

Agterberg FP, Cheng Q, Brown A, Good D (1996) Multifractal modeling of fractures in the Lac du Bonnet batholith, Manitoba. Computers & Geosciences 22 (5) : 497-507. https://doi.org/10.1016/0098-3004(95)00117-4

Aissaoui D (1984) Les structures liées à l'accident sud-atlasique entre Biskra et le Djebel Manndra, Algérie. Évolution géométrique et cinématique. Ph.D. Dissertation thesis. Universityof Strasbourg .

Allegre CJ, Le Mouel JL, Provost A (1982) Scaling rules in rock fracture and possible implications for earthquake prediction. Nature 297:47-49. https://doi.org/10.1038/297047a0

Arneodo A, Grasseau G, Holschneider M (1988) Wavelet transform of multifractals. Physical review letters 61(20):2281. https://doi.org/10.1103/PhysRevLett.61.2281

Arneodo A, Bacry E, Muzy JF (1995) the thermodynamics of fractals revisited with wavelets. Physica A: Statistical Mechanics and its Applications 213(1-2):232-275. https://doi.org/10.1016/0378-4371(94)00163-N

Arneodo A, Jaffard S (2004) L'analyse multi-fractale des signaux. Journal du CNRS 107.

Arneodo A, Audit B, Kestener P, Roux S (2008) Wavelet-based multifractal analysis. Scholarpedia 3(3):4103. 10.4249/scholarpedia.4103

Bacry E, Muzy JF, Arneodo A (1993) Singularity spectrum of fractal signals from wavelet analysis: Exact results. Journal of statistical physics 70:635-674. https://doi.org/10.1007/BF01053588

Barenblatt GI, Zheltov IP, Kochina IN (1960) Basic concepts in the theory of seepage of homogeneous liquids in fissured rocks [strata]. Journal of applied mathematics and mechanics 24(5):1286-1303. https://doi.org/10.1016/0021-8928(60)90107-6

Barton CC (1995) Fractal analysis of scaling and spatial clustering of fractures. In :La Pointe PR (eds) Fractals in the earth sciences. Springer, Boston. pp 141–178. https://doi.org/10.1007/978-1-4899-1397-5_8

Basirat R, Goshtasbi K, Ahmadi M (2019) Determination of the fractal dimension of the fracture network system using image processing technique. Fractal and Fractional 3(2):17. https://doi.org/10.3390/fractalfract3020017

Berkowitz B, Hadad A (1997) Fractal and multifractal measures of natural and synthetic fracture networks. Journal of Geophysical Research: Solid Earth 102(B6):12205-12218. https://doi.org/10.1029/97JB00304

Berkowitz B (2002) Characterizing flow and transport in fractured geological media: A review. Advances in water resources 25(8-12):861-884.https://doi.org/10.1016/S0309-1708(02)00042-8

Bonnet E, Bour O, Odling NE, Davy P, Main I, Cowie P, Berkowitz B (2001) Scaling of fracture systems in geological media. Reviews of geophysics 39(3):347-383. https://doi.org/10.1029/1999RG000074

Boudjema A (1987) Évolution structurale du bassin pétrolier" triasique" du Sahara Nord oriental (Algérie). Ph.D. Dissertation thesis .University of Paris 11.

Bour O, Davy P (1999) Clustering and size distributions of fault patterns: Theory and measurements. Geophysical Research Letters 26(13):2001-2004. https://doi.org/10.1029/1999GL900419

Bureau D (1986) Approche sédimentaire de la dynamique structurale. Evolution mésozoïque et devenir orogénique de la partie septentrionale du fossé saharien (Sud-Ouest constantinois et Aurès, Algérie). Ph.D. dissertation thesis .University of Paris 6.

Busson G (1970) Le Mésozoïque saharien. 2ème partie : Essai de synthèse des données des sondages algéro-tunisiens. CNRS, Paris.

Cacas MC, Ledoux E, de Marsily G, Tillie B, Barbreau A, Durand E, Feuga B, Peaudecerf P (1990) Modeling fracture flow with a stochastic discrete fracture network: calibration and validation: 1. The flow model. Water Resources Research 26(3):479-489. https://doi.org/10.1029/WR026i003p00479

Caire A (1975) Essai de coordination des accidents transversaux en Algérie et en Tunisie. Comptes Rendus de l'Académie des Sciences 280 : 403-406.

Cantor G (1884) De la puissance des ensembles parfaits de points: Extrait d'une lettre adressée à l'éditeur. Acta Mathematica 4(1):381-392. https://doi.org/10.1007/BF02418423

Castaing C, Halawani MA, Gervais F, Chilès JP, Genter A, Bourgine B, Ouillon G, Brosse JM, Martin P, Genna A, Janjou D (1996) Scaling relationships in intraplate fracture systems related to Red Sea rifting. Tectonophysics 261(4) :291-314. https://doi.org/10.1016/0040-1951(95)00177-8

Chilès JP (1988) Fractal and geostatistical methods for modeling of a fracture network. Mathematical Geology 20:631-654.https://doi.org/10.1007/BF00890581

Cinco H, Miller FG, Ramey JrH.J (1975) Unsteady-state pressure distribution created by a directionally drilled well. Journal of Petroleum Technology 27(11):1392-1400. https://doi.org/10.2118/5131-PA

Cornet A (1959) Sur la fosse sud-aurésienne. Comptes Rendus de la société géologique de France .

Cowie PA, Sornette D, Vanneste C (1995) Multifractal scaling properties of a growing fault population. Geophysical Journal International 122(2):457-469. https://doi.org/10.1111/j.1365-246X.1995.tb07007.x

Darcel C, Bour O, Davy P (2003) Cross-correlation between length and position in real fracture networks. Geophysical Research Letters 30(12). https://doi.org/10.1029/2003GL017174

Davy P, Sornette A, Sornette D (1990) Some consequences of a proposed fractal nature of continental faulting. Nature 348(6296):56-58.https://doi.org/10.1038/348056a0

De Bartolo SG, Gaudio R, Gabriele S (2004) Multifractal analysis of river networks: Sandbox approach. Water resources research 40(2). https://doi.org/10.1029/2003WR002760

De Souza J, Rostirolla SP (2011) A fast MATLAB program to estimate the multifractal spectrum of multidimensional data: Application to fractures. Computers & Geosciences 37(2):241-249. https://doi.org/10.1016/j.cageo.2010.09.001

Dverstop B, Andersson J (1989) Application of the discrete fracture network concept with field data: Possibilities of model calibration and validation. Water Resources Research 25(3):540-550.https://doi.org/10.1029/WR025i003p00540

Evertsz CJG, Mandelbrot BB (1992) Multifractal measures. In: Peitgen HO, Jurgens H, Saupe D (eds) Chaos and fractals, Appendix B. Springer Verlag, New York, pp849-881.

Feder J (1988) The Fractal Dimension. In: Fractals. Physics of Solids and Liquids. Springer, Boston, MA, pp 6-30. https://doi.org/10.1007/978-1-4899-2124-6_2

Field DJ (1987) Relations between the statistics of natural images and the response properties of cortical cells. Josa a 4(12):2379-2394. https://doi.org/10.1364/JOSAA.4.002379

Frizon de Lamotte D, Ghandriche H, Moretti I (1990) La flexure saharienne : trace d'un chevauchement aveugle post-pliocène de flèche plurikilométrique au Nord du Sahara. (Aurès, Algérie). Comptes rendus de l'Académie des sciences Série 2. Mécanique, Physique, Chimie, Sciences de l'univers, Sciences de la Terre 310(11):1527-1532.

Gauthier BDM, Lake SD (1993) Probabilistic modeling of faults below the limit of seismic resolution in Pelican Field, North Sea, offshore United Kingdom. AAPG bulletin 77(5):761-777.https://doi.org/10.1306/BDFF8D4E-1718-11D7-8645000102C1865D

Ghandriche H (1991) Modalités de la superposition de structures de plissement-chevauchement d'âge alpin dans les Aurès (Algérie). Ph.D. Dissertation thesis .University of Paris 11.

Ghosh A, Daemen JJ (1993) Fractal characteristics of rock discontinuities. Engineering geology 34(1-2):1-9. https://doi.org/10.1016/0013-7952(93)90039-F

Gilman JR (2003) Practical aspects of simulation of fractured reservoirs. In International Forum on Reservoir Simulation. Buhl, Baden-Baden, Germany, pp 23-27.

Gonzato G (1998) A practical implementation of the box counting algorithm. Computers & Geosciences 24(1):95-100. https://doi.org/10.1016/S0098-3004(97)00137-4

Grassberger P (1983) Generalized dimensions of strange attractors. Physics Letters A 97(6):227-230. https://doi.org/10.1016/0375-9601(83)90753-3

Grassberger P (1993) On efficient box counting algorithms. International Journal of Modern Physics C 4(03):515-523. https://doi.org/10.1142/S0129183193000525

Grazzini J, Turiel A, Yahia H, Herlin I (2007) A multifractal approach for extracting relevant textural areas in satellite meteorological images. Environmental Modelling & Software 22(3):323-334. https://doi.org/10.1016/j.envsoft.2005.07.032

Grazzini J, Soille P (2009) Edge-preserving smoothing using a similarity measure in adaptive geodesic neighbourhoods. Pattern Recognition 42(10):2306-2316. https://doi.org/10.1016/j.patcog.2008.11.004

Gringarten AC, Ramey JrHJ (1974) Unsteady-state pressure distributions created by a well with a single horizontal fracture, partial penetration, or restricted entry. Society of petroleum engineers journal 14(04):413-426. https://doi.org/10.2118/3819-PA

Gringarten AC, Ramey JrHJ, Raghavan R (1974) Unsteady-state pressure distributions created by a well with a single infinite-conductivity vertical fracture. Society of Petroleum Engineers Journal 14(04): 347-360.https://doi.org/10.2118/4051-PA

Guiraud R (1973) Evolution post-triasique de l'avant-pays de la chaîne alpine en Algérie. Ph.D. Dissertation thesis. University of Toulouse.

Guiraud R (1975) L'évolution post-triasique de l'avant pays de la chaîne alpine en Algérie, d'après l'étude du bassin du Hodna et des régions voisines. Rev. Geogr. Phys. Geol. Dynam17 :427-446.

Halsey TC, Meakin P, Procaccia I (1986) Scaling structure of the surface layer of diffusion-limited aggregates. Physical review letters 56(8):854. https://doi.org/10.1103/PhysRevLett.56.854

Harte D (2001) Multifractals: theory and applications. Chapman and Hall/CRC, New York https://doi.org/10.1201/9781420036008

Hirata T, Imoto M (1991) Multifractal analysis of spatial distribution of micro earthquakes in the Kanto region. Geophysical Journal International 107(1):155-162. https://doi.org/10.1111/j.1365-246X.1991.tb01163.x

Hsieh PA, Shapiro AM, Barton CC, Haeni FP, Johnson CD, Martin CW, Pailett FL, Winter TC, Wright DL (1993) Methods of Characterizing Fluid Movement and Chemical Transport in Fractured Rock. *Field Trip Guidebook for the Northeastern United States, 2*, R1-R30. https://corescholar.libraries.wright.edu/ees/90

Huang F, Yao C, Zhang X, Shao Y, He C, Zhou C (2020a) Connectivity evaluation for three‐dimensional fracture network in support‐based model: A case study in the Ordos Basin, China. Energy Science & Engineering 8(7):2492-2510. https://doi.org/10.1002/ese3.681

Huang F, Yao C, Yang J, He C, Shao Y, Zhou C (2020b) Connectivity evaluation of fracture networks considering the correlation between trace length and aperture. Applied Mathematical Modelling 88:870-887. https://doi.org/10.1016/j.apm.2020.07.011

Jenkins DN, Prentice JK (1982) Theory for aquifer test analysis in fractured rocks under linear (nonradial) flow conditions. Groundwater 20(1) :12-21. https://doi.org/10.1111/j.1745-6584.1982.tb01325.x

Kazi-Tani N (1986) Evolution géodynamique de la bordure nord-africaine: le domaine intraplaque nord-algérien: approche megaséquentielle. Ph.D. Dissertation thesis .University of Pau.

Laffitte R (1939) Les plissements post-nummulitiques dans l'Atlas saharien. Société Géologique de France.

Lasm T, Razack M (2001) Lois d'échelle dans la fracturation de roches dures cristallines et dans le réseau hydrographique associé. Comptes Rendus de l'Académie des Sciences-Series IIA-Earth and Planetary Science 333(4):225-232. https://doi.org/10.1016/S1251-8050(01)01632-9

Lausberg C (1987) Calcul numérique de la dimension fractale d'un attracteur étrange. Ph.D. Dissertation thesis. University of Grenoble-INPG .

Lévy Véhel J (2000) Analyse Fractale: une nouvelle génération d'outils pour le Traitement du Signal. Revue des Sciences et Technologies de l'Information-Série TSI: Technique et Science Informatiques 19(1-3):335-350 https://hal.inria.fr/inria-00578649/

LévyVéhel J (2003) Fractal and multifractal processing of images. Traitement du Signal 20(3):303. https://core.ac.uk/download/pdf/15486515.pdf

LévyVéhel J, Barrière O (2008) Local Holder regularity-based modeling of RR intervals. In 2008 21st IEEE International Symposium on Computer-Based Medical Systems. Jyvaskyla, Finland .10.1109/CBMS.2008.65

Liu X, Srinivasan S, Wong D (2002) Geological characterization of naturally fractured reservoirs using multiple point geostatistics. In SPE/DOE Improved Oil Recovery Symposium. Tulsa, Oklahoma. https://doi.org/10.2118/75246-MS

Long CS, Billaux DM (1987) From Field data to fracture network modelling : an example incorporating spatial structure Water resources research 23(7) :1201-1216. https://doi.org/10.1029/WR023i007p01201

Lopes R, Betrouni N (2009) Fractal and multifractal analysis: a review. Medical image analysis 13(4):634-649. https://doi.org/10.1016/j.media.2009.05.003

Mallat S, Zhong S (1991) Wavelet transform maxima and multiscale edges. Wavelets and Their Applications. ed MB Ruskai.

Mallat S (1998) Applied mathematics meets signal processing. In Proceedings of the Challenges for the 21st century. Papers from the international conference on fundamental sciences: mathematics and theoretical physics, pp. 138-161. http://eudml.org/doc/226897

Mandelbrot BB (1974) Intermittent turbulence in self-similar cascades: divergence of high moments and dimension of the carrier. Journal of fluid Mechanics 62(2):331-358. https://doi.org/10.1017/S0022112074000711

Mandelbrot BB (1975) Les objets fractals: forme, hasardet dimension. Flammarion, Paris.

Mandelbrot BB (1982) the fractal geometry of nature. WH freeman, New York

Mandelbrot BB (1989) Multifractal Measures, Especially for the Geophysicist. In: Scholz CH, Mandelbrot BB (eds) Fractals in Geophysics. Pure and Applied Geophysics. Birkhäuser, Basel, pp 5-42. https://doi.org/10.1007/978-3-0348-6389-6_2

Mariethoz G Renard P, Caers J (2010) Bayesian inverse problem and optimization with iterative spatial resampling. Water Resources Research 46(11). https://doi.org/10.1029/2010WR009274

Marrett R, Allmendinger RW (1991) Estimates of strain due to brittle faulting: sampling of fault populations. Journal of Structural Geology 13(6):735-738.https://doi.org/10.1016/0191-8141(91)90034-G

Muzy JF, Bacry E, Arneodo A (1991) Wavelets and multifractal formalism for singular signals: Application to turbulence data. Physical review letters 67(25):3515. https://doi.org/10.1103/PhysRevLett.67.3515

Neretnieks I (1993) Solute Transport in Fractured Rock-Applications to Radioactive Waste Repositories. In : Bear J, Tsang CF, de Marsily G Flow and Contaminant Transport in Fractured Rocks . Elsevier, Academic Press, pp 39-127. https://doi.org/10.1016/B978-0-12-083980-3.50006-1

Odling NE (1992) Network properties of a two-dimensional natural fracture pattern. Pure and Applied Geophysics 138:95-114.https://doi.org/10.1007/BF00876716.

Odling NE, Gillespie P, Bourgine B, Castaing C, Chiles JP, Christensen NP, Fillion E, Genter A ,Olsen C, Thrane L , Trice R, Aarseth E, Walsh JJ, Watterson, J (1999) Variations in fracture system geometry and their implications for fluid flow in fractures hydrocarbon reservoirs. Petroleum Geoscience 5(4):373-384. https://doi.org/10.1144/petgeo.5.4.373.

Olsen L (1995) A multifractal formalism. Advances in mathematics 116(1):82-196. https://doi.org/10.1006/aima.1995.1066.

Olsson O (1992) Site characterization and validation-Final Report (No. STRIPA-TR--92-22). Swedish Nuclear Fuel and Waste Management Co.

Ouillon G, Sornette D, Castaing C (1995) Organisation of joints and faults from 1-cm to 100-km scales revealed by optimized anisotropic wavelet coefficient method and multifractal analysis. Nonlinear Processes in Geophysics 2(3/4):158-177. https://doi.org/10.5194/npg-2-158-1995.

Parisi G, Frisch U (1985) A multifractal model of intermittency. In :Ghil MR, Benzi R, Parisi G (Eds). Turbulence and predictability in geophysical fluid dynamics and climate dynamics. North Holland, pp 84-88.

Pavičić I, Dragičević I, Vlahović T, Grgasović T (2017) Fractal analysis of fracture systems in upper Triassic dolomites in Žumberak Mountain, Croatia. Rudarsko-geološko-naftnizbornik 32(3):1 -13. https://hrcak.srce.hr/183707 .

Peitgen HO, Jürgens H, Saupe D, Feigenbaum MJ (2004) Chaos and fractals: new frontiers of science. Springer, New York.

Potirakis SM, Eftaxias K, Kopanas J, Antonopoulos G (2012) Signatures of the self-affinity of fracture and faulting in pre-seismic electromagnetic emissions. arXiv preprint arXiv:1211.5113. https://doi.org/10.48550/arXiv.1211.5113.

Razack M (1984) Application de méthodes numériques et statistiques à l'identification des réservoirs fissurés carbonates en hydrodéologie. Ph.D. Dissertation thesis. University of Sciences and Techniques of Languedoc .

Razack M, Lasm T (2006) Geostatistical estimation of the transmissivity in a highly fractured metamorphic and crystalline aquifer (Man-Danane Region, Western Ivory Coast). Journal of Hydrology 325(1-4):164-178. https://doi.org/10.1016/j.jhydrol.2005.10.014.

Roux S, Hansen A (1990) Introduction to multifractality. In: Charmet JC, Guyon E, Roux S (eds) Disorder and fracture (NATO Science Series B, 235), pp 17-30.

Russell DA, Hanson JD, Ott E (1980) Dimension of strange attractors. Physical Review Letters 45(14):1175. https://doi.org/10.1103/PhysRevLett.45.1175

Secrieru C (2009) Applications de l'analyse fractale dans le cas de ruptures dynamiques. Ph.D. Dissertation thesis. Arts et Métiers Paris Tech.

Shapiro AM, Hsieh PA (1996) Overview of Research on Use of Hydrologic, Geophysical, and Geochemical Methods to Characterize Flow and Chemical Transport in Fractured Rock at the Mirror Lake Site, New Hampshire. In: Morganwalp DW, Aronson DA (eds) US Geological Survey Toxic Substances Hydrology Program—Proceedings of the Technical Meeting, Colorado Springs, Colorado, pp 71-80.

Srivastava RM, Frykman P, Jensen M (2004) Geostatistical Simulation of Fracture Networks. In: Leuangthong O, Deutsch CV (eds) Geostatistics Banff 2004. Quantitative Geology and Geostatistics, Springer, Dordrecht, pp 295-304. https://doi.org/10.1007/978-1-4020-3610-1_30

Thiéry D, Vandenbeusch M, Vaubourg P (1983) Interprétation des pompages d'essai en milieu fissuré aquifère .BRGM. https://hal-brgm.archives-ouvertes.fr/hal-01062367.

Thrailkill J (1988) Drawdown interval analysis: a method of determining the parameters of shallow conduit flow carbonate aquifers from pumping tests. Water Resources Research 24(8):1423-1428. https://doi.org/10.1029/WR024i008p01423 .

Tsang CF, Neretnieks I (1998) Flow channeling in heterogeneous fractured rocks. Reviews of Geophysics 36(2):275-298. https://doi.org/10.1029/97RG03319.

Turiel A, Grazzini J, Yahia H (2005) Multiscale techniques for the detection of precipitation using thermal IR satellite images. IEEE Geoscience and Remote Sensing Letters 2(4):447-450. 10.1109/LGRS.2005.852712

Turiel A, Pérez-Vicente CJ, Grazzini J (2006) Numerical methods for the estimation of multifractal singularity spectra on sampled data: A comparative study. Journal of Computational Physics 216(1):362-390. https://doi.org/10.1016/j.jcp.2005.12.004

Verscheure M, Fourno A, Chilès JP (2010) History matching of a stochastic multifractal subesismic fault model. In ECMOR XII-12th European Conference on the Mathematics of Oil Recovery. European Association of Geoscientists & Engineers.https://doi.org/10.3997/2214-4609.20144967 .

Vila JM (1980) La chaîne alpine d'Algérie orientale et des confins Algéro-Tunisiens. Ph.D. Dissertation thesis. University of Pierre et Marie curie.

Walsh JJ, Watterson J (1993) Fractal analysis of fracture patterns using the standard box-counting technique: valid and invalid methodologies. Journal of structural Geology 15(12):1509-1512. https://doi.org/10.1016/0191-8141(93)90010-8.

Wang W, Zheng S, Lian R, Liang Y (2017) Rock fissure pattern characterization by combining 1-D fractal dimension and statistical analysis. IEEE/CAA Journal of Automatica Sinica. 10.1109/JAS.2017.7510391.

Warren JE, Root PJ (1963) The behavior of naturally fractured reservoirs. Society of Petroleum Engineers Journal 3(03):245-255.https://doi.org/10.2118/426-PA.

Weiss J (2003) Scaling of fracture and faulting of ice on earth. Surveys in Geophysics 24:185-227. https://doi.org/10.1023/A:1023293117309.

Wendt, H, Abry P, Roux SG, Jaffard S (2007) Analyse multifractaled'images: l'apport des coefficients dominants.GRETSI. http://hdl.handle.net/2042/28803

Witherspoon PA (2000) Investigations at Berkeley on Fracture Flow in Rocks: From the Parallel Model to Chaotic System. In: Faybishenko B, Witherspoon PA, and Benson SM (eds) Dynamics of Fluids in Fractured Rock. Washington, pp 1-72.

Wornell G (1996) Signal processing with fractals: a wavelet-based approach. Prentice Hall Press

Zazoun RS, Marok A, Samar L, Benadla M, Mezlah H (2015) Fracturing and deformation bands in the El Kohol area (Central Saharan Atlas, Algeria): fractal analysis, scaling laws and discrete fracture network modelling. EstudiosGeológicos 71(2):e039. http://dx.doi.org/10.3989/egeol.42011.359

Table

Table 1 Calculation of the fractal dimension using the box counting method of the lineament maps

n	Boxes size in pixels	Number of boxes (non-empty)			
		Es=1/200000	Es=1/100000	Es=1/50000	Es=1/25000
0	$2^0 = 1$	461314	445448	412300	408830
1	$2^1 = 2$	124852	122948	118363	116874
2	$2^2 = 4$	32767	32755	32710	32659
3	$2^3 = 8$	8192	8192	8192	8192
4	$2^4 = 16$	2048	2048	2048	2048
5	$2^5 = 32$	512	512	512	512
6	$2^6 = 64$	128	128	128	128
7	$2^7 = 128$	32	32	32	32
8	$2^8 = 256$	8	8	8	8
9	$2^9 = 512$	2	2	2	2
10	$2^{10} = 1024$	1	1	1	1

Figures

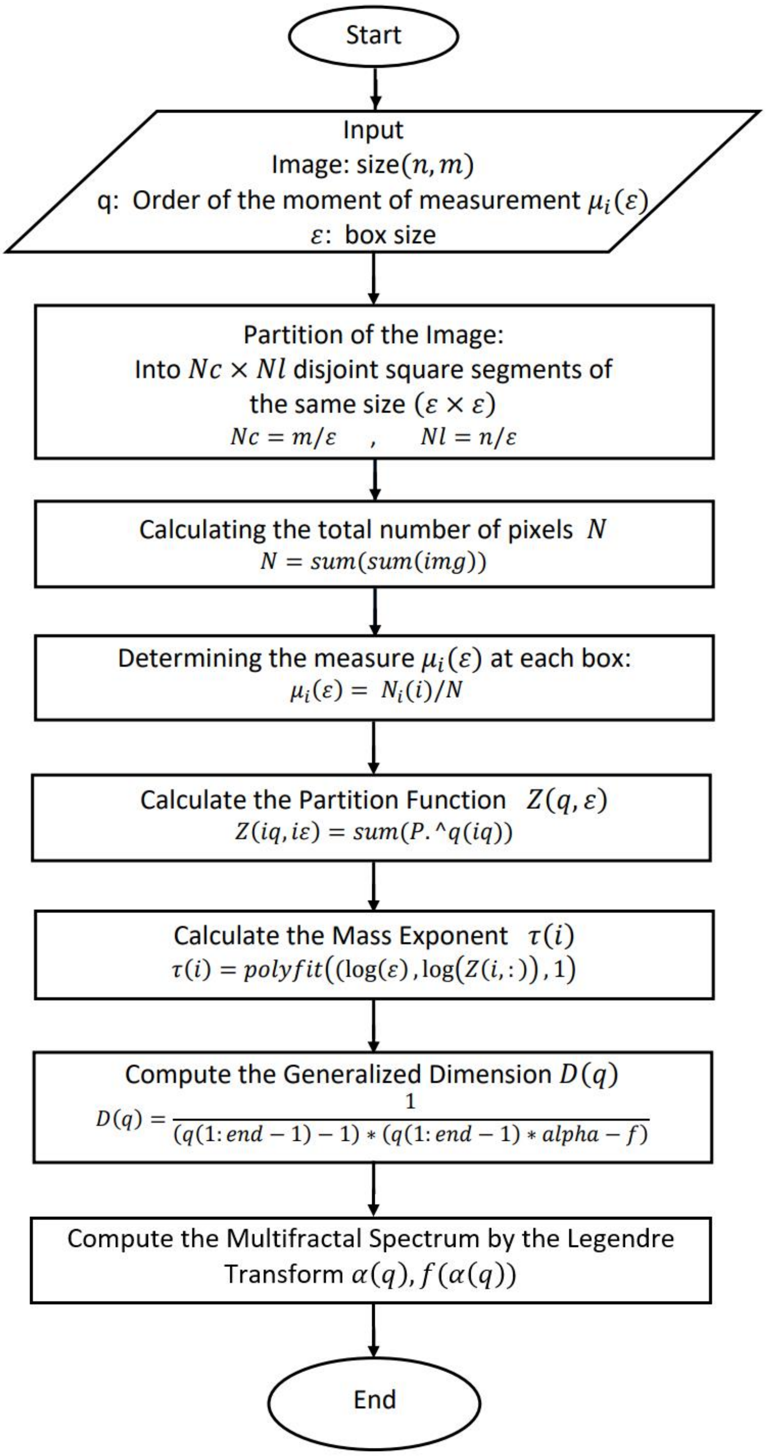

Fig. 1 2D-MAFN flowchart of the calculation code for the multifractal analysis of fracture networks.

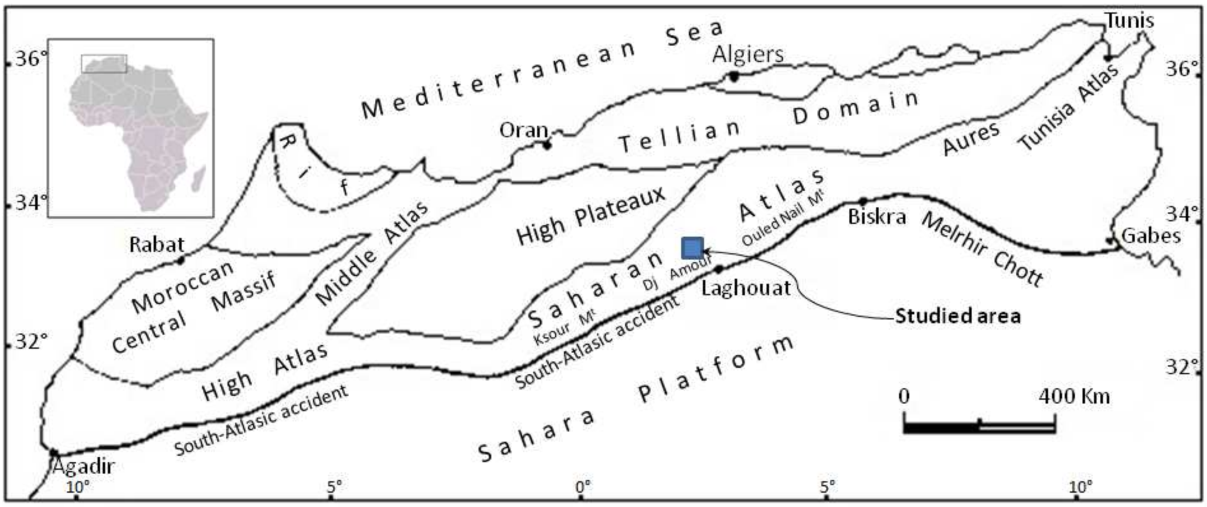

Fig. 2 Main structural domains from the Maghreb region in North Africa and location of the study area

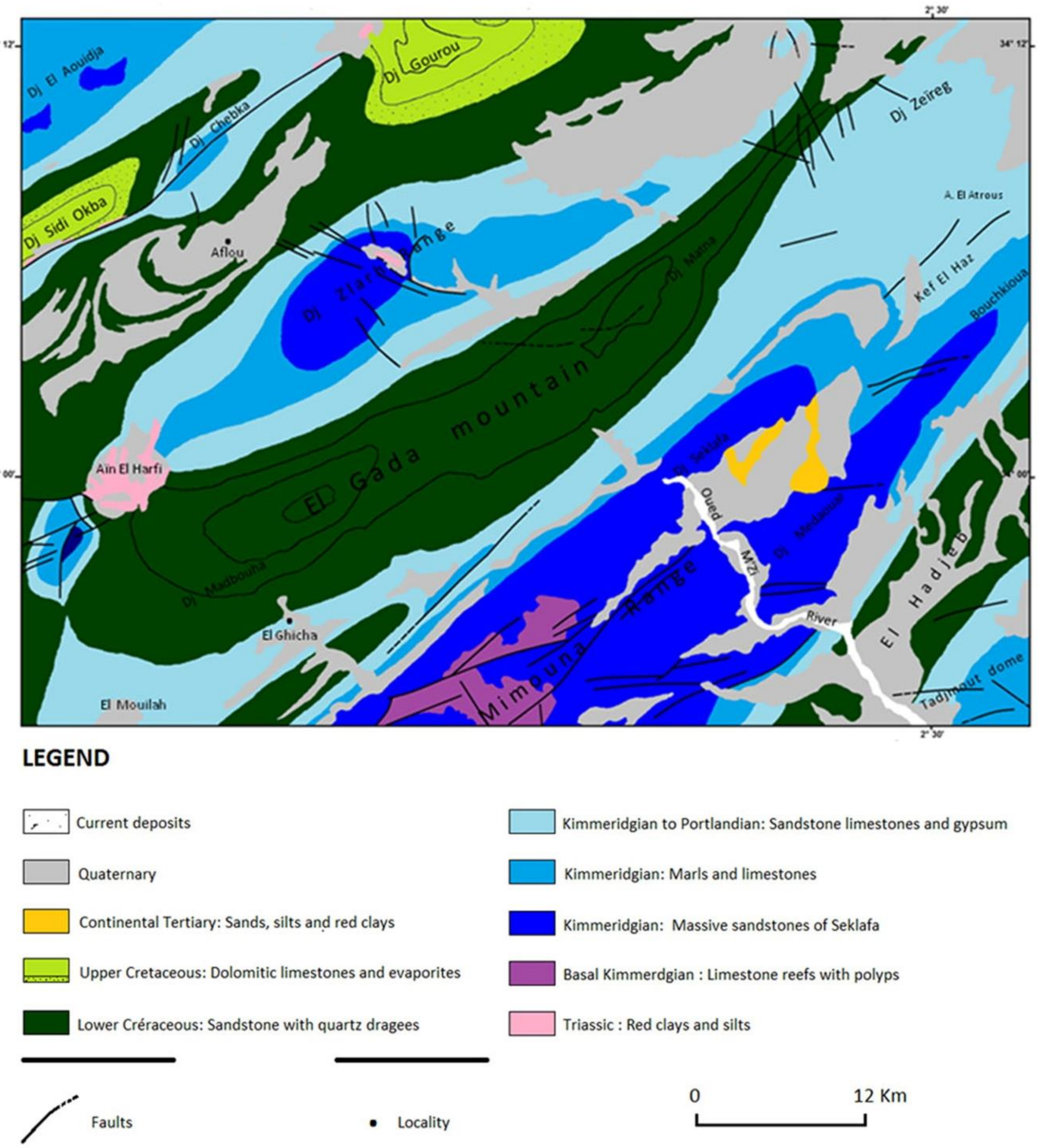

Fig. 3 Geological map of the study area of the El Gada region

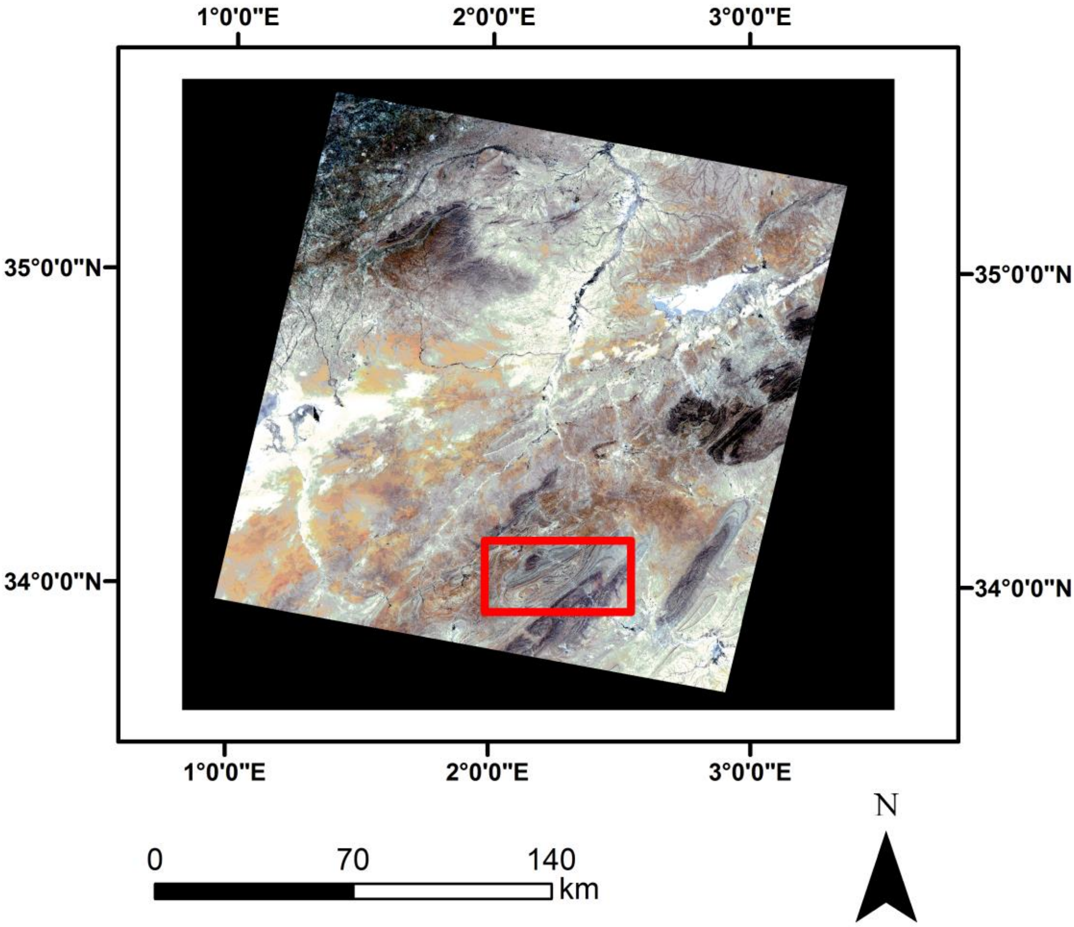

Fig. 4 Landsat 7 ETM+ scene, channels 3, 2 and 1 in RGB covering the study area

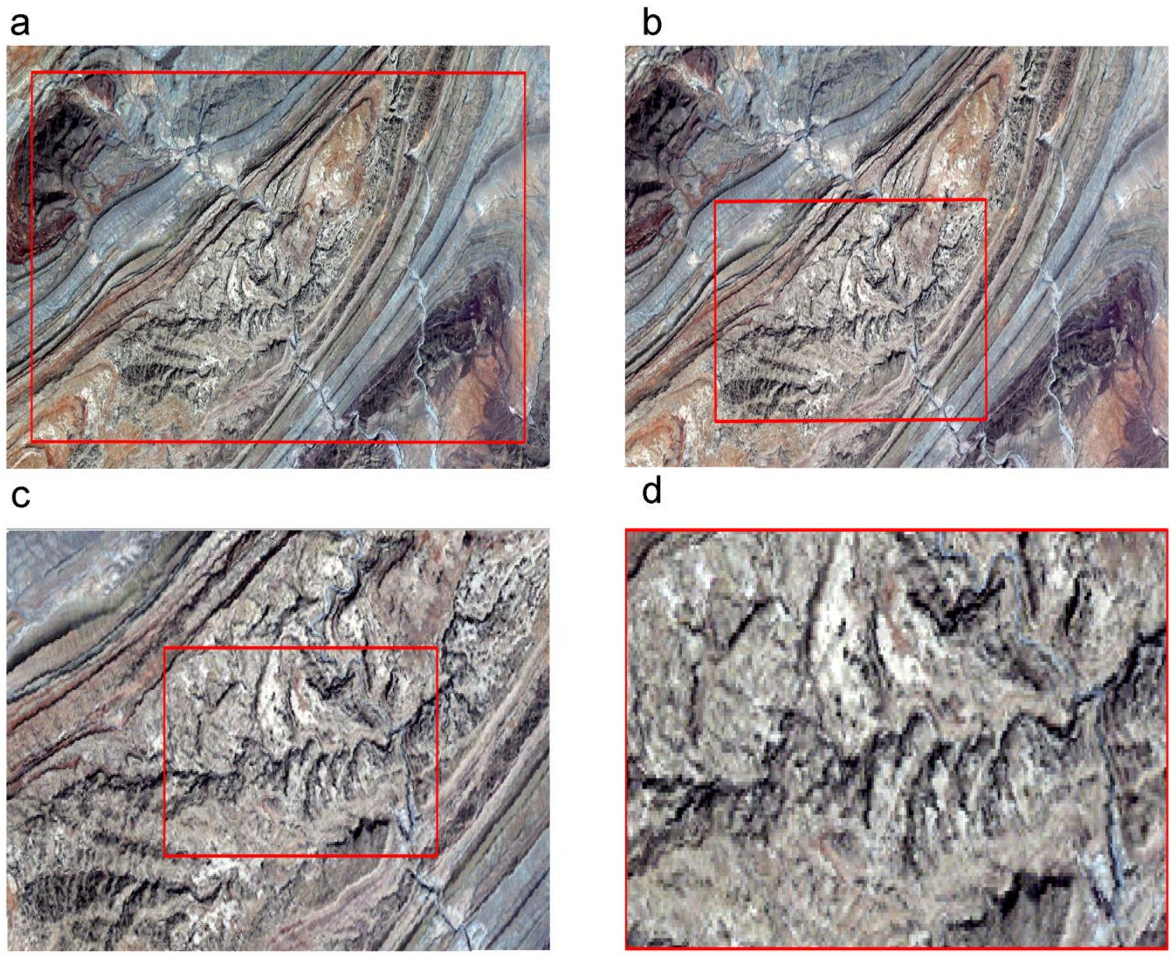

Fig. 5 Natural color images 321 RGB to the scales: (a) 1/200 000, (b) 1/100 000, (c) 1/50 000 and (d) 1/25 000

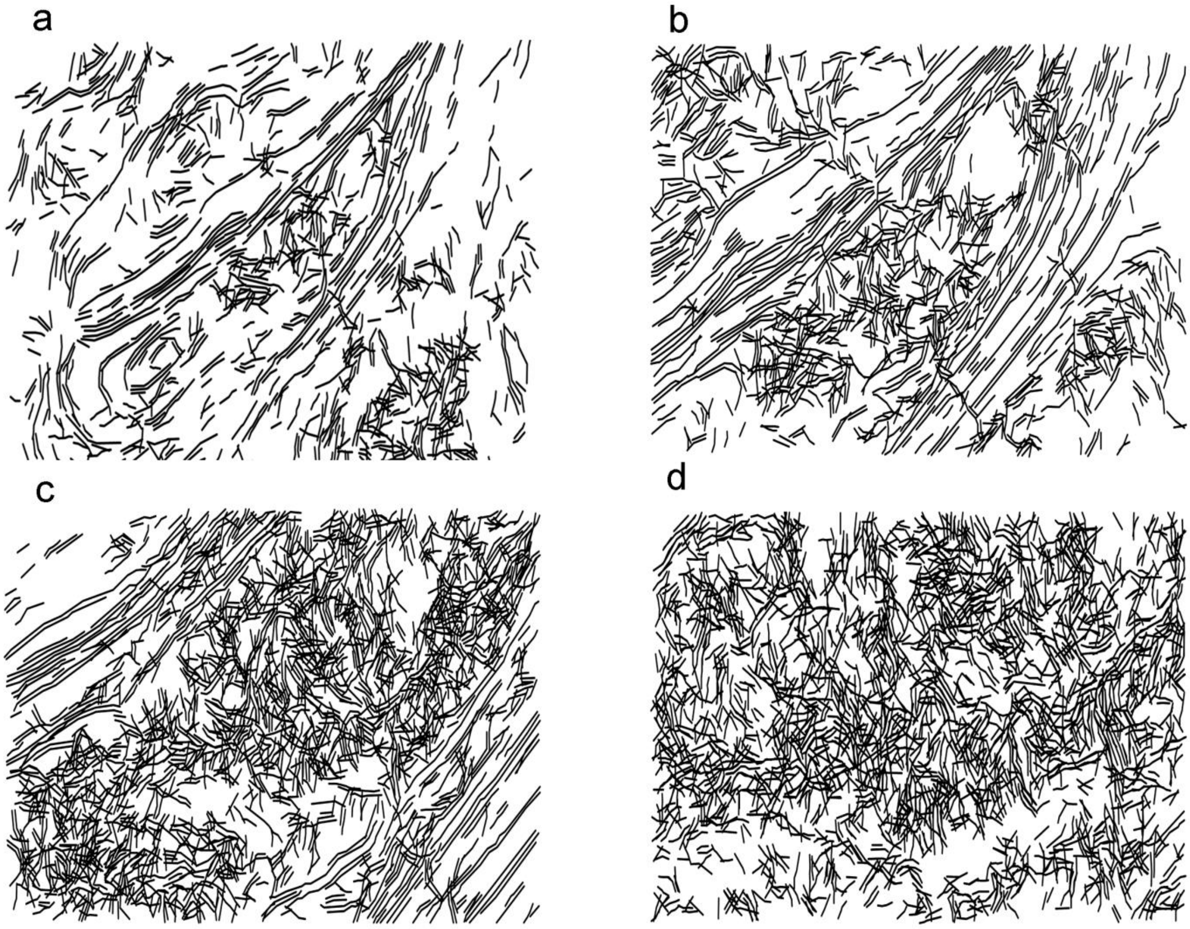

Fig. 6 Lineament synthesis maps of the El Gada region, to the scales: (a) 1/200 000, (b) 1/100 000, (c) 1/50 000 and (d) 1/25 000

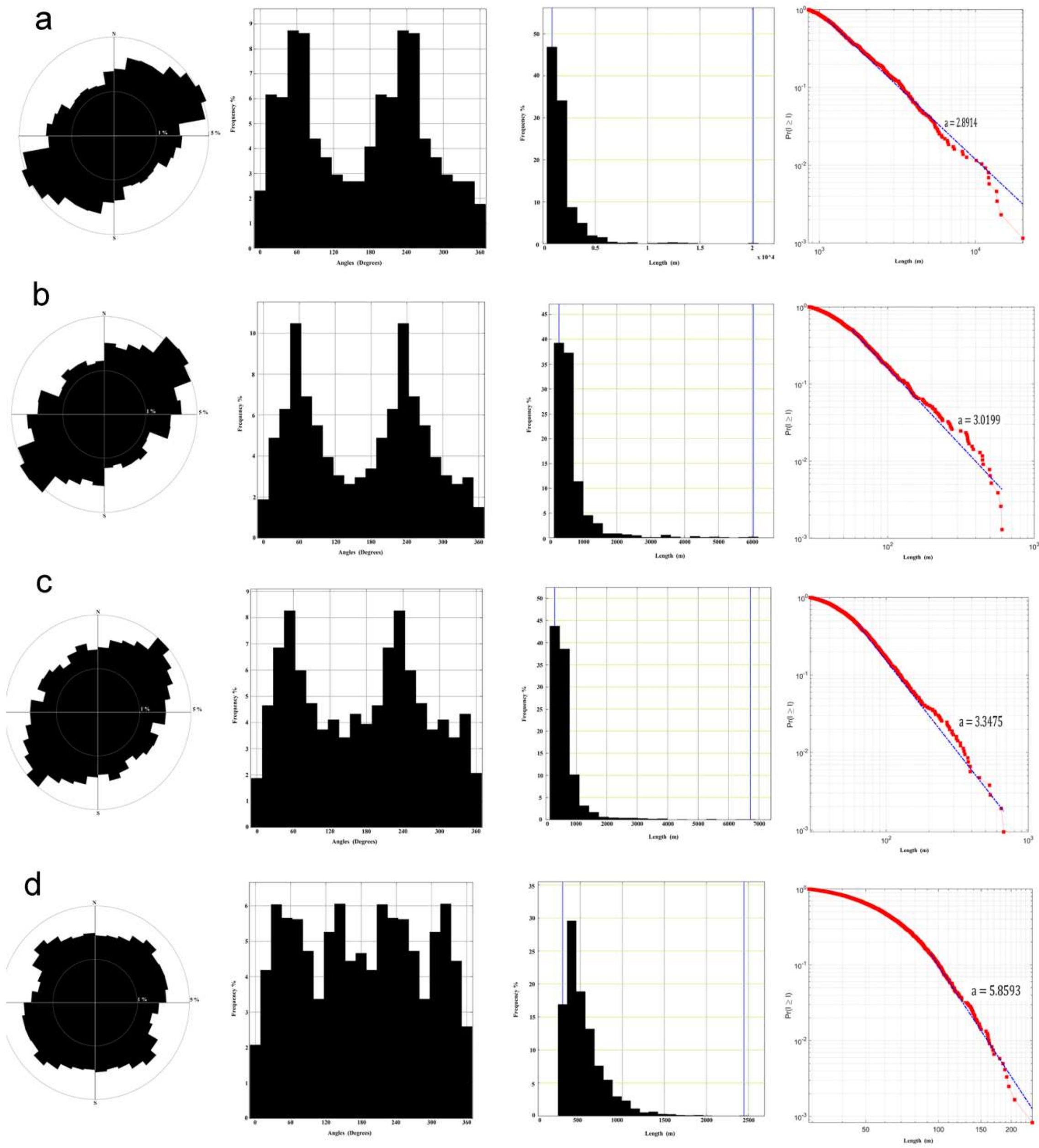

Fig.7 Results of the geometric analysis of the lineament networks.From left to right: Lineament network rose diagrams, Histograms of orientation angles, Histograms of lineament length frequencies and Power Law fitting of the lineament length distribution using the Maximum Likelihood estimators to the scales: (a) 1/200,000, (b) 1/100,000, (c) 1/50,000 and (d) 1/25,000.

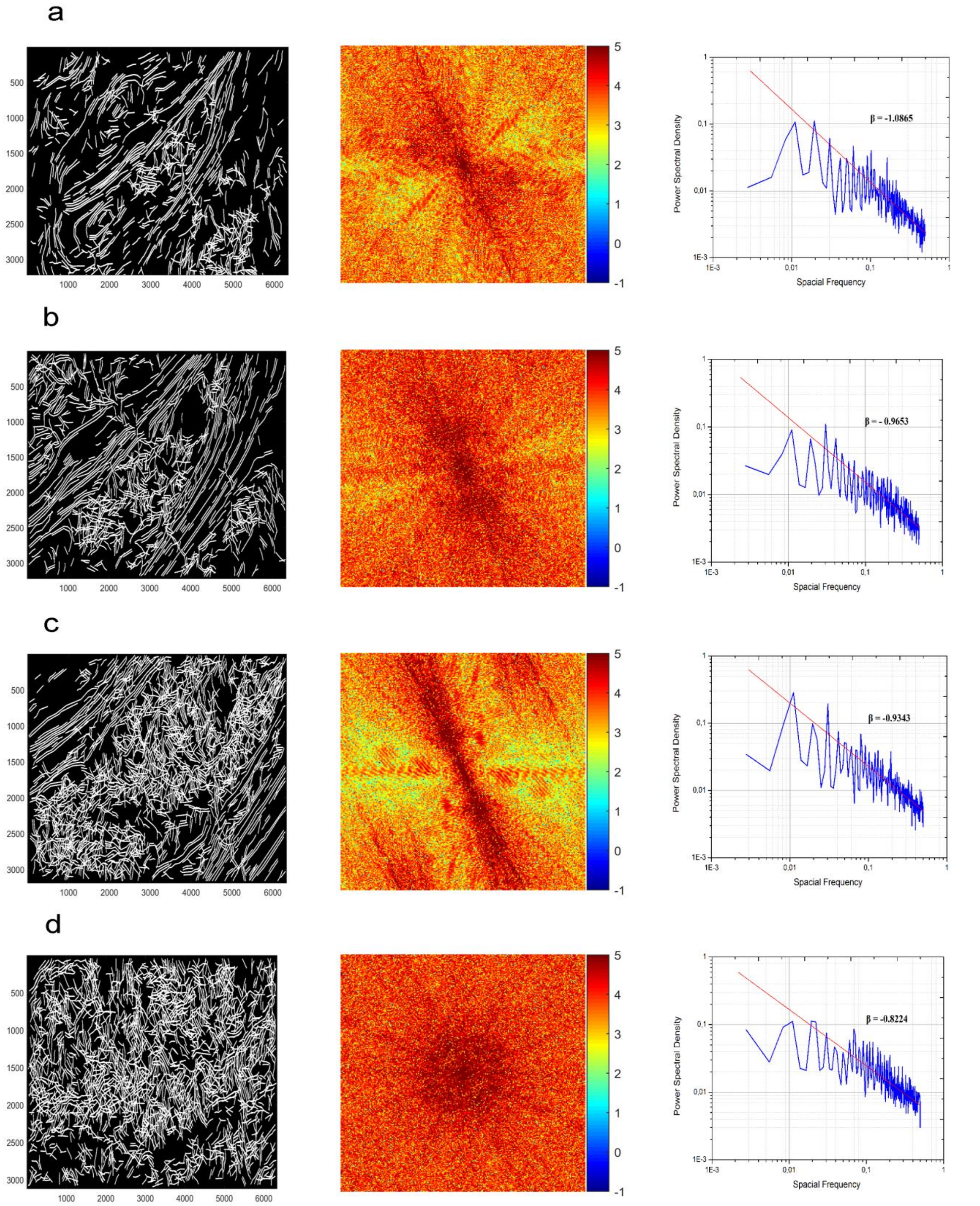

Fig.8Illustration of scale invariance on the power spectrum.From left to right: Binary image of the lineament map, Log-scale power spectral density and log−log plot of power spectral density with the spatial frequency to the scales: (a) 1/200 000, (b) 1/100 000, (c) 1/50 000 and (d) 1/25 000

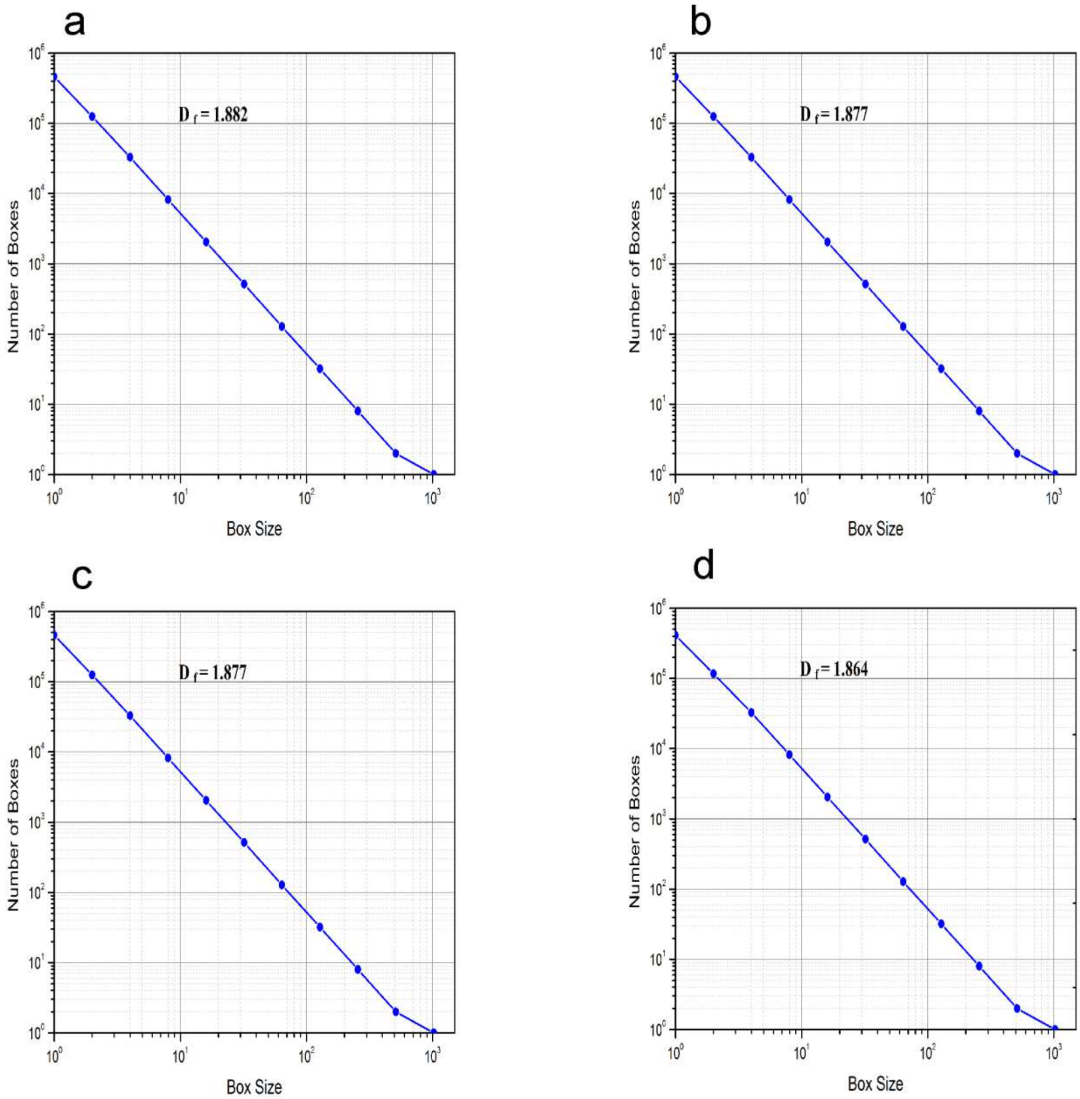

Fig.9 Estimation of the Fractal Dimension of lineament maps to the scales:
(a) 1/200 000, (b) 1/100 000, (c) 1/50 000 and (d) 1/25 000

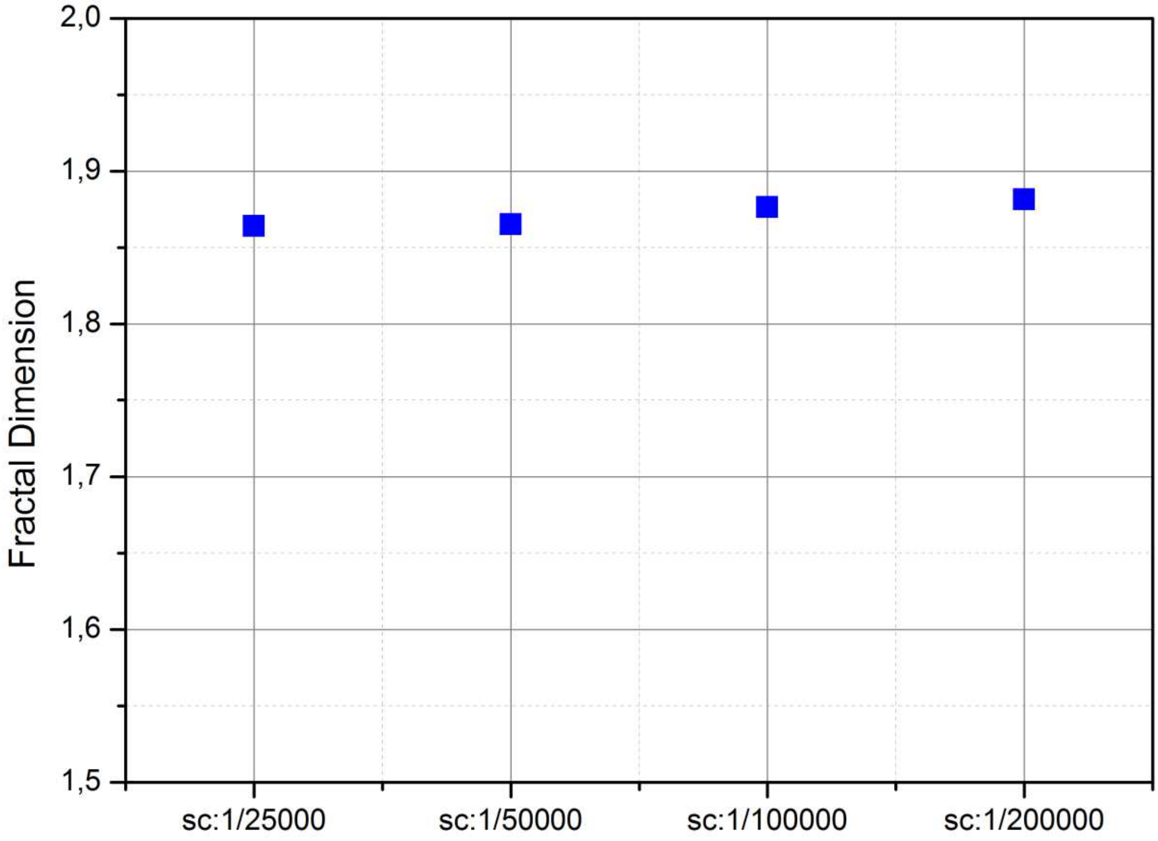

Fig 10.Fractal dimensions calculated for each of the lineament maps of the study area at different scales

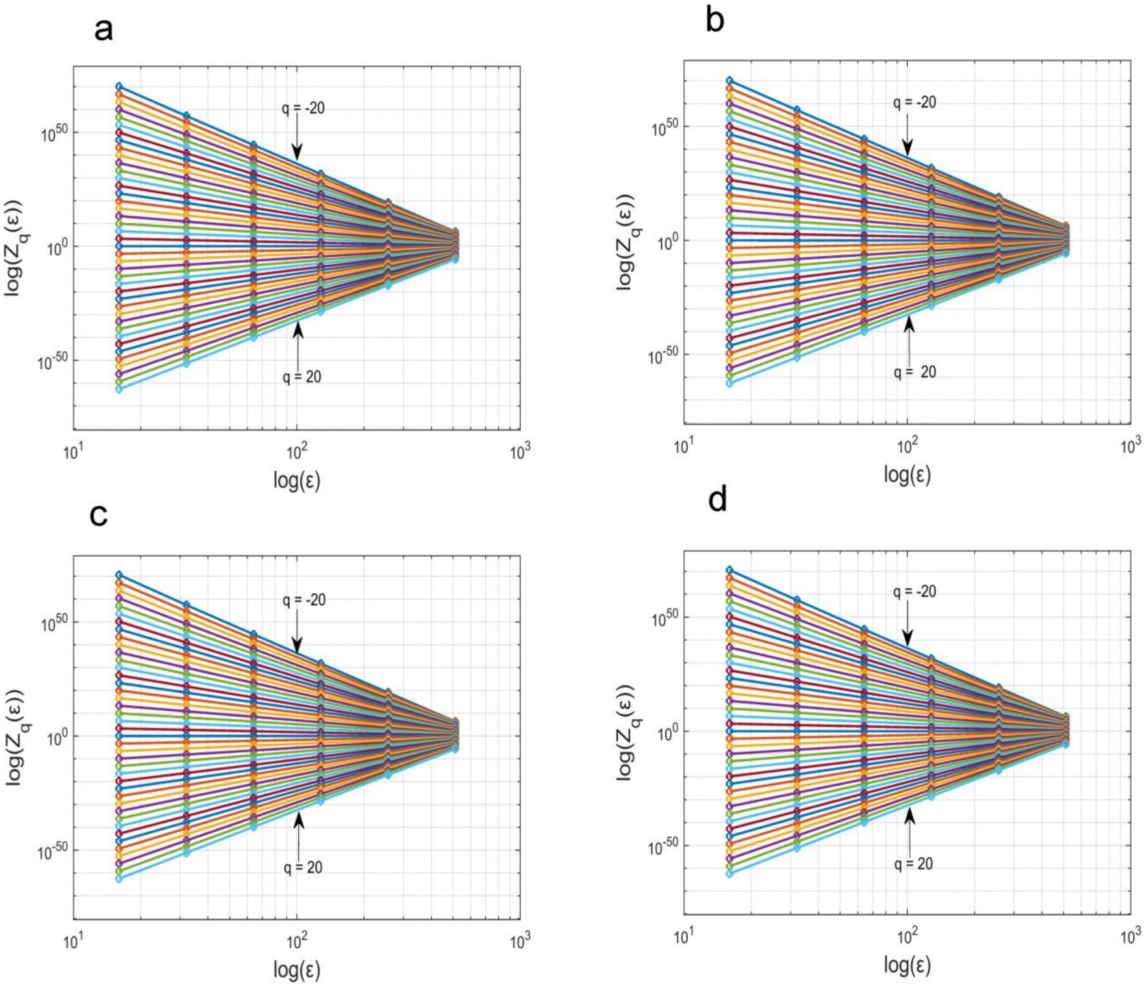

Fig.11 Log-log plot of mass partition function $Z(q, \varepsilon)$ versus scale $(\varepsilon)$of lineament maps to the scales: (a) 1/200 000, (b) 1/100 000, (c) 1/50 000 and (d) 1/25 000

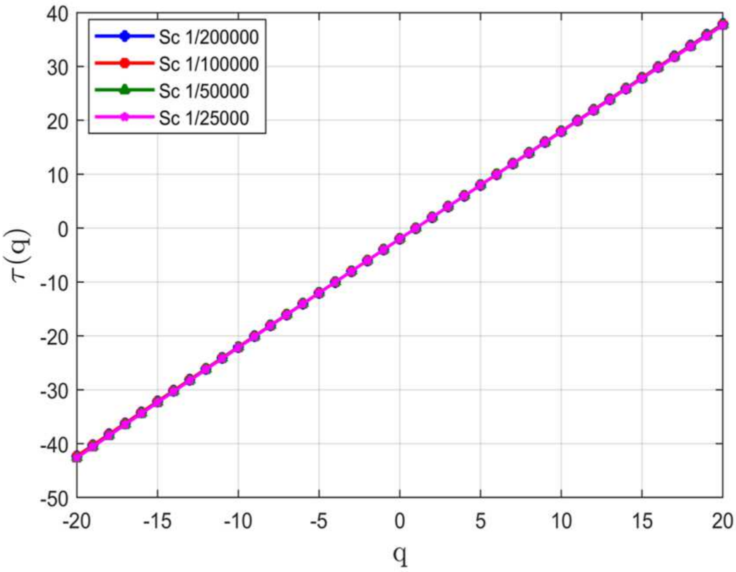

Fig. 12 Relationship between mass exponent $\tau(q)$and moment $q$of lineament maps

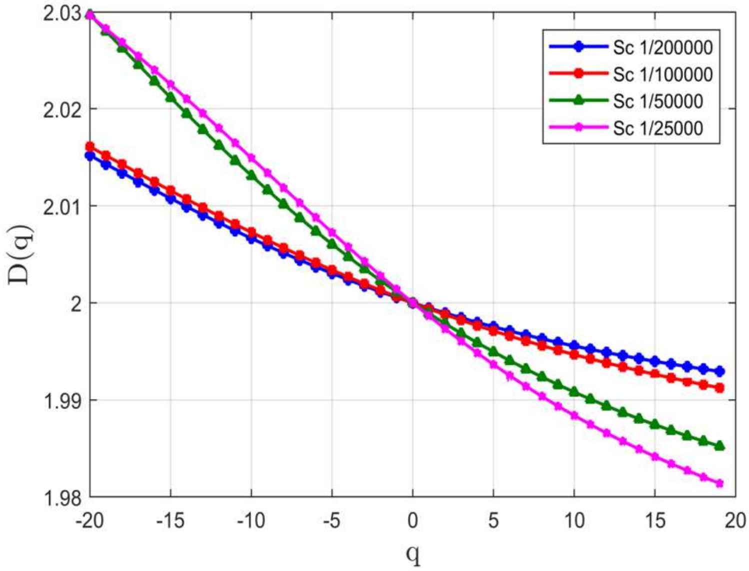

Fig. 13 Relationship between singularity exponent $D(q)$ and moment $q$of lineament maps

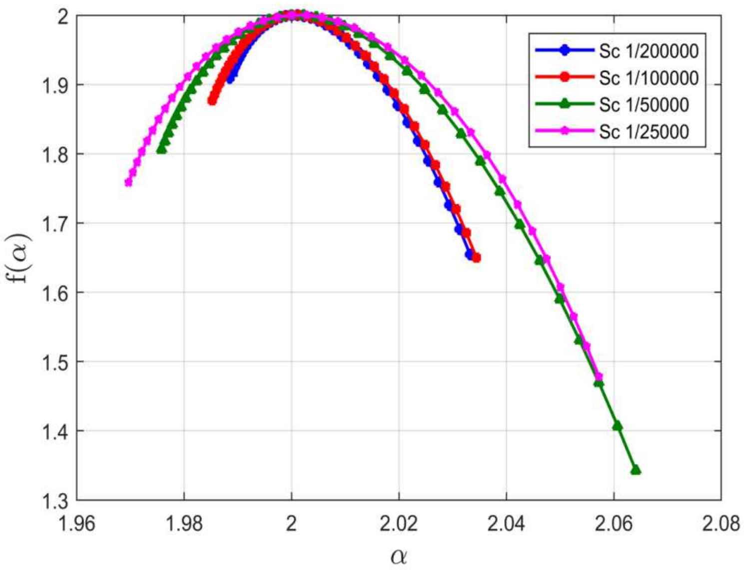

Fig. 14 Relationship between multifractal spectrum $f(\alpha)$ and singularity exponent $\alpha$of lineament maps